Journal of Geophysical Research: Atmospheres

RESEARCH ARTICLE
10.1029/2018JD028338

Background Free-Tropospheric Ice Nucleating Particle Concentrations at Mixed-Phase Cloud Conditions

Larissa Lacher[1,2], Paul J. DeMott[3], Ezra J. T. Levin[3], Kaitlyn J. Suski[3,4], Yvonne Boose[1,5], Assaf Zipori[6,7], Erik Herrmann[8], Nicolas Bukowiecki[8], Martin Steinbacher[9], Ellen Gute[10], Jonathan P. D. Abbatt[10], Ulrike Lohmann[1], and Zamin A. Kanji[1]

[1]Institute for Atmospheric and Climate Science, ETHZ, Zurich, Switzerland, [2]Now at Atmospheric Aerosol Research, Institute for Meteorology and Climate Research, KIT, Karlsruhe, Germany, [3]Department of Atmospheric Science, Colorado State University, Fort Collins, CO, USA, [4]Now at Pacific Northwest National Laboratory, Richland, WA, USA, [5]Now at Institute for Atmospheric Physics, German Aerospace Center, Oberpfaffenhofen-Wessling, Germany, [6]Institute for Earth Science, Hebrew University, Jerusalem, Israel, [7]Now at Department of Earth and Planetary Sciences, Weizmann Institute of Science, Rehovot, Israel, [8]Laboratory of Atmospheric Chemistry, Paul Scherrer Institute, Villigen, Switzerland, [9]Empa, Swiss Federal Laboratories for Materials Science and Technology, Duebendorf, Switzerland, [10]Department of Chemistry, University of Toronto, Toronto, Ontario, Canada

Key Points:
- Background free-tropospheric INP concentrations at 242 K in the immersion mode measured at the High Altitude Research Station Jungfraujoch reach a maximum interquartile range of 10 INP/stdL
- Agreement with INP concentrations under similar measurement conditions but in different locations in the free troposphere also suggests ~10 INP/stdL regardless of location
- No seasonal variability in INP concentrations in the background free troposphere is observed at the High Altitude Research Station Jungfraujoch

Correspondence to:
L. Lacher and Z. A. Kanji,
larissa.lacher@kit.edu;
zamin.kanji@env.ethz.ch

Citation:
Lacher, L., DeMott, P. J., Levin, E. J. T., Suski, K. J., Boose, Y., Zipori, A., et al. (2018). Background free-tropospheric ice nucleating particle concentrations at mixed-phase cloud conditions. *Journal of Geophysical Research: Atmospheres*, *123*, 10,506–10,525. https://doi.org/10.1029/2018JD028338

Received 16 JAN 2018
Accepted 8 AUG 2018
Accepted article online 21 AUG 2018
Published online 18 SEP 2018

Abstract Clouds containing ice are vital for precipitation formation and are important in determining the Earth's radiative budget. However, primary formation of ice in clouds is not fully understood. In the presence of ice nucleating particles (INPs), the phase change to ice is promoted, but identification and quantification of INPs in a natural environment remains challenging because of their low numbers. In this paper, we quantify INP number concentrations in the free troposphere (FT) as measured at the High Altitude Research Station Jungfraujoch (JFJ), during the winter, spring, and summer of the years 2014–2017. INPs were measured at conditions relevant for mixed-phase cloud formation at $T = 241/242$ K. To date, this is the longest timeline of semiregular measurements akin to online INP monitoring at this site and sampling conditions. We find that INP concentrations in the background FT are on average capped at 10/stdL (liter of air at standard conditions [$T = 273$ K and $p = 1013$ hPa]) with an interquartile range of 0.4–9.6/stdL, as compared to measurements during times when other air mass origins (e.g., Sahara or marine boundary layer) prevailed. Elevated concentrations were measured in the field campaigns of 2016, which might be due to enhanced influence from Saharan dust and marine boundary layer air arriving at the JFJ. The upper limit of INP concentrations in the background FT is supported by measurements performed at similar conditions, but at different locations in the FT, where we find INP concentrations to be below 13/stdL most of the time.

1. Introduction

Only a small fraction of the atmosphere is composed of clouds, but their interactions with shortwave and longwave radiation influence the Earth's radiative budget considerably (Boucher et al., 2013). In the assessment of anthropogenic climate change, the role of mixed-phase clouds (MPCs), consisting of water in all three phases, is more uncertain than that of warm clouds (Lohmann, 2017). In addition, precipitation formation is most efficient in MPCs (Rogers & Yau, 1989) and most precipitation is formed via the ice phase (Lau & Wu, 2003; Lohmann & Feichter, 2005; Mülmenstädt et al., 2015). However, understanding the formation and development of MPCs has remained largely uncertain in atmospheric science, due to the complex nature of the system (Korolev et al., 2017). Part of this uncertainty is associated with microphysical properties and a limited understanding of the origin of ice crystals in MPCs. To date, immersion/condensation freezing is viewed to be the most important primary freezing mechanism for MPCs (Ansmann et al., 2008; de Boer et al., 2011; Westbrook & Illingworth, 2013), where the phase change from ice to water is triggered by an ice nucleating particle (INP) within a supercooled liquid droplet. In addition, contact freezing, where an INP triggers ice formation upon contact with the water-air interface of a supercooled cloud droplet, might also be relevant to MPC formation (Ladino Moreno et al., 2013; Nagare et al., 2016; Seifert et al., 2011).

The understanding of primary ice formation in MPCs is further complicated by the possible contribution of different INP types. Within the free troposphere (FT), an environment in which MPCs occur, only 1 out of 10^5–10^6 aerosol particles act as an INP (e.g., DeMott et al., 2010; Rogers et al., 1998). This renders the

identification and quantification of INPs challenging. INP species relevant for the formation of ice in MPCs include mineral dust particles, such as desert dust and soil dust (also containing organic matter/biogenic components), bio-aerosols (pollen, bacteria, fungi, lichens, and exudates from phytoplankton), volcanic ashes, and combustion aerosol particles (summarized in Kanji et al., 2017). However, surface emissions can be transported into the FT via convection, entrainment, and subsequent (long-range) advection. This is because the FT is decoupled from direct surface forcing, like frictional drag, emission of aerosol particles and trace gases, and terrain-induced flow modification. Such forcings typically change on time scales of an hour or less (Stull, 1988). Therefore, aerosol particles present in the FT are either newly formed by gas-to-particle conversion or are emitted from the boundary layer and injected and transported in the FT, when aerosol particles can undergo atmospheric aging (e.g., Pöschl, 2005), such as chemical reactions and surface coatings, or cloud processing (e.g., Hoose et al., 2008). This might, in turn, affect the ice nucleation ability of INPs (Kanji et al., 2017). For example, China et al. (2017) observed that the majority of INPs sampled in the FT were coated by organic material and that the temperature and relative humidity (RH) at which ice first forms on these particles varies only by 5%, despite different chemical composition of the INPs, source regions, and transport patterns.

In order to advance our understanding of ice nucleation in the FT, continuous monitoring of INP concentrations is required. Suitable platforms for FT sampling are aircraft based or high-altitude stations, where FT conditions prevail. However, influence from the local boundary layer or anthropogenic emissions can perturb the FT at such locations over time intervals of tens of minutes to hours (e.g., Herrmann et al., 2015). This limits filter sampling techniques with subsequent ice nucleation experiments to quantify purely FT INP concentrations, because the time scale of temporal changes in FT INP concentrations may at times limit the effectiveness for sampling bulk volumes. These methods have their greatest benefits for assessing the most efficient INPs through collection over long sample periods (e.g., Ardon-Dryer & Levin, 2014; Bigg, 1967; Bingemer et al., 2012; Conen et al., 2011; Knopf et al., 2014; Mason, Chou et al., 2015; Santachiara et al., 2010). INP sampling with high temporal resolution on the order of minutes is achieved with online techniques such as Continuous Flow Diffusion Chambers (CFDCs; Rogers, 1988), which determine INP concentrations at a set temperature and supersaturation condition (Chou et al., 2011; DeMott et al., 2010). To date, however, CFDCs cannot be operated autonomously and need a human interface, resulting in high temporal resolution measurements of INP concentrations being limited to single-field campaigns. A handful ambient INP measurements under FT conditions do exist (Ardon-Dryer & Levin, 2014; Bigg, 1967; Boose, Kanji et al., 2016; Boose, Sierau et al., 2016; Conen et al., 2015; DeMott, Sassen, et al., 2003; DeMott et al., 2010; Field et al., 2012; Lacher et al., 2017; Mason, Si, et al., 2015; Prenni et al., 2009; Richardson et al., 2007; Rogers et al., 1998; Schrod et al., 2017; Stith et al., 2009). These studies find that in the temperature range 238–243 K, INP concentrations span several orders of magnitude, from <1 to several hundred INPs per standard liter of air (per stdL, given at standard conditions of T = 273.15 K and pressure = 1,013 hPa). However, to our knowledge, no study on the seasonality of INP concentrations in the background FT exists. Conen et al. (2015) measured INP concentrations at the High Altitude Research Station (JFJ), Switzerland, at temperatures warmer than in this study (i.e., 265 K), and a seasonal cycle in INP concentrations was found, with INP concentrations ranging between 10^{-3} and 10^{-2}/stdL. The seasonality observed was attributed to boundary layer influence, and thus, the measurements do not represent FT conditions. In this work we present background FT INP measurements at 241–242 K at the JFJ during different seasons (winter, spring, and summer) and years (2014–2017) to investigate possible seasonal and annual differences. In addition, we compare our results to other measurements in the FT, at different locations, to show similarities in the magnitude of the global FT background INP concentration.

2. Methods

2.1. Location and Time of Field Campaigns

Field campaigns were conducted at the High Altitude Research Station Jungfraujoch (JFJ), located in the Bernese Alps (3,580 m above sea level; 46°33′N, 7°59′E). The JFJ is a Global Atmospheric Watch (GAW) monitoring station and part of the ACTRIS2 Infrastructure (European Research Infrastructure for the observation of Aerosol, Clouds, and Trace gases), the Swiss National Air Pollution Monitoring Network (NABEL), and the SwissMetNet meteorological network. Aerosol physical properties (e.g., Baltensperger et al., 1997;

Table 1
Overview of Field Campaigns Conducted at the JFJ From Winter 2014 to Winter 2017

			All	BLI	FT_{all}	$FT_{background}$	SDE	Marine event
Campaign	Start	End	Sampling time (h)	% of time	% of time	% of time	#/(%)	#/(%)
All campaigns	-	-	514.8	43	57	51	5/(2)	12/(5)
Winter 2014	24.01.	26.02.	27.9	72	27	27	1	0
Summer 2014	13.08.	27.08.	15.9	62	38	38	0	0
Winter 2015	24.01.	09.02.	23.4	13	87	65	1	2
Spring 2015	17.05.	29.06.	55.8	47	53	52	1	1
Summer 2015	31.07.	12.08.	32.1	91	9	9	0	0
Winter 2016	13.01.	06.03.	99	26	74	55	2	4
Spring 2016	21.05.	14.06.	49.8	86	14	9	0	3
Summer 2016	01.08.	21.08.	99.3	55	45	37	0	2
Winter 2017	22.01.	21.02.	111.6	8	92	92	0	0

Note. Sampling times for all measurements are given in hours along with respective percentages for the occurrence of BLI, FT_{all}, and $FT_{background}$; occurrence of SDEs and marine events are given as numbers of events and percentages of occurrence of time. BLI, boundary layer injection; FT, free troposphere; JFJ, High Altitude Research Station Jungfraujoch; SDE, Saharan dust event.

Bukowiecki et al., 2016) and trace gases (Steinbacher et al., 2016) are monitored and accompanied by measurements of meteorological conditions (Appenzeller et al., 2008).

Throughout the year, the site is surrounded by firn ice and rocks and does not experience noticeable influence from local vegetation but can be affected by daytime tourist activities (summarized in Bukowiecki et al., 2016) and related work on the infrastructure of the station and tunnel systems. Due to its elevation, the JFJ experiences undisturbed FT conditions for most of the time during winter (e.g., Herrmann et al., 2015) and thus represents background aerosol concentrations (Baltensperger et al., 1997). During the warmer season, the site can be influenced by boundary layer injections (BLIs), which reach the site by thermally induced lifting, synoptical lifting, and lifting due to Föhn events (Collaud Coen et al., 2011; Griffiths et al., 2013; Herrmann et al., 2015; Lugauer et al., 1998; Zellweger et al., 2003). This results in a seasonal cycle of aerosol particle concentration and population, as well as air mass origins. In addition, the JFJ is regularly influenced by Saharan dust events (SDEs) transported within the FT (Collaud Coen et al., 2004), as well as air masses which originated in the marine boundary layer (Boose, Kanji, et al., 2016; Cui et al., 2011; Lacher et al., 2017).

Measurements of INP concentrations at temperature and RH conditions typical for MPCs were carried out in several campaigns between 2014 and 2017 (see Table 1 in section 3.1). The duration of each campaign was two to five weeks and took place in winter (January, February, and beginning of March), spring (May and June), and summer (end of July and August).

2.2. Ice Nucleation Measurements

Measurements of INP number concentrations in this study represent exclusively condensation/immersion freezing mode. In winter 2014 INP sampling was performed with the CFDC, PINC (Portable Ice Nucleation Chamber) at T = 241 K and RH_w (RH with respect to water) = 103% (RH with respect to ice [RH_i] = 141%), and temperature and RH uncertainties of ±0.4 K and ±2%, respectively. INPs were exposed to these conditions for 5 s. Details on the characterization, working principle, and field setup can be found in Chou et al. (2011) and Boose, Kanji et al. (2016). Since summer 2014, INP concentrations were measured with HINC (Horizontal Ice Nucleation Chamber), a CFDC that is described in detail by Lacher et al. (2017). HINC measurements were performed at T = 242 K and RH_w = 104% (RH_i = 140%), with uncertainties in temperature and RH_w of ±0.4 K and ±1.5%, respectively, and a residence time of 8 s. The choice of supersaturation in the two CFDCs was determined so that all particles entering the chamber experience $RH_w > 100\%$ due to a variation of RH in the aerosol layer (DeMott et al., 2015; Lacher et al., 2017). The measurement temperature was considerably colder than the ambient temperature at the JFJ. As such the measured INP concentrations at the JFJ represent those that nucleate ice in a temperature range between ambient temperature, and 242 K, since a depletion of INP active at temperatures warmer than ambient is expected (Conen et al., 2016; Stopelli et al., 2015)

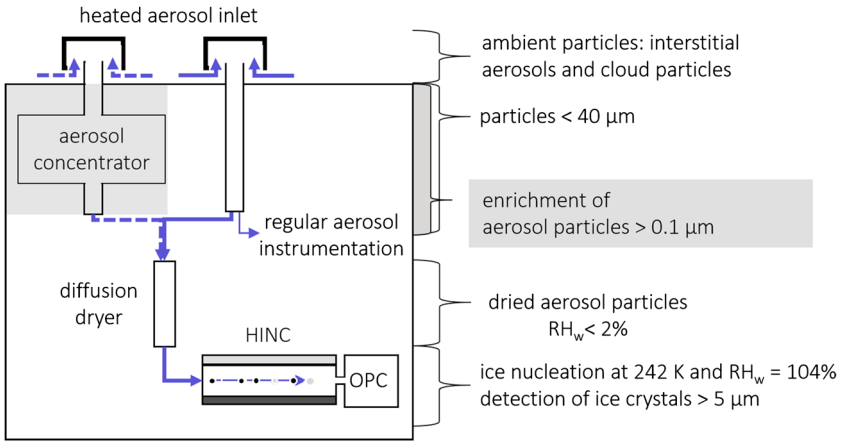

Figure 1. Setup of ice nucleation experiments at the High Altitude Research Station Jungfraujoch during summer 2014 to summer 2016 (flow direction: blue solid line) and with the aerosol concentrator (PAPC) in winter 2017 (grey shaded area; flow direction dashed blue line).

prior to the air mass reaching the JFJ. During the study, ambient temperatures were between 272 and 267 K (interquartile range during the sampling times of INPs in all conditions and all field campaigns), and the difference up to 242 K is a typical range for the occurrence of MPCs (e.g., Bühl et al., 2016).

The setup of HINC as used at the JFJ is depicted in Figure 1. Aerosol particles were sampled through the GAW total aerosol particle inlet (Weingartner et al., 1999), which had a size cutoff of 40 µm in diameter and was heated to 298 K to evaporate sampled cloud particles. The aerosol particle transmission efficiency in the inlet system and the ice chamber is 56% for particles <2 µm (see Lacher et al., 2017, for more detail). As such INP measurements are representative for aerosol particles in this size range, which is characteristic for ambient particles at the JFJ (Baltensperger et al., 1997; Nyeki et al., 1998). Before entering HINC, the aerosol flow was guided through a diffusion dryer to reduce the RH_w to $<2\%$. Measurements were performed in and out of clouds, which did not significantly influence INP concentrations at given measurement conditions and location (Boose, Kanji et al., 2016).

For comparison between INP concentrations and other measurements, the lowest time resolution was used to which the measurements with the higher time resolution were averaged.

INP number concentrations were continuously monitored using measurement periods of 20 min. Before and after each such sample measurement, background measurements were conducted to determine any internally formed ice (noise), which can be misclassified as INPs. Ambient INP concentrations were calculated as the difference between the INP concentrations derived during the sample measurements and the background (filtered air) measurements. The chamber background concentration from filtered air also determined the instrument's limit of detection. The determination of the limit of detection follows Poisson statistics, for which a detailed description can be found in Lacher et al. (2017).

To normalize INP concentrations to the available surface area of the ambient aerosol population per unit volume (A_{tot}), the ice-active surface site density, n_s (m^{-2}), is calculated as $=INP/A_{tot}$ (Hoose & Möhler, 2012). A_{tot} was obtained from a Scanning Mobility Particle Sizer (SMPS), measuring in the size range 20–600 nm, and an optical particle counter (OPC, GRIMM Dust Monitor 1.108), measuring in the size range 0.23–2 µm (both given in volume equivalent diameter; Herrmann et al., 2015). This size range is representative for particles sampled with HINC (Lacher et al., 2017). The SMPS consists of a differential mobility analyzer (DMA, TSI 3071) and a condensation particle counter (CPC, TSI, 3775). The OPC and SMPS have a time resolution of 1 and 6 min, respectively. For comparison to the INP measurements, averages over the INP time resolution were considered.

The naturally low INP numbers in the midtroposphere challenge INP quantification with online detection methods. To increase the signal-to-noise ratio in HINC, the portable aerosol particle concentrator (PAPC) from the University of Toronto was applied upstream of HINC in winter 2017. The PAPC was operated at a separate custom-built heated aerosol inlet, identical to the GAW total aerosol particle inlet. The working principle of

the PAPC is based on the virtual impaction method (Sioutas et al., 1995) and increases the number concentration of ambient particles depending on their physical size, resulting in aerosol particle enhancement factors (EF_{aero}) less than 3 (for diameters [d] < 0.1 μm) and up to 20 (for d = 0.5–2.5 μm; see Figure A1 in the appendix). The PAPC's upper size cutoff is lower than the GAW total inlet cutoff size. However, this difference is not of concern in the light of the low abundance of particles >2 μm at the sampling site (Baltensperger et al., 1997; Nyeki et al., 1998) and that HINC only samples particles <2 μm. The EF_{aero} is constant for a given size. In order to determine an INP enrichment factor (EF_{INP}), which might not be constant due to varying sizes of INPs, measurements with HINC were performed downstream of the concentrator inlet ($INP_{concentrator}$) and periodically downstream of the GAW total inlet (INP_{total}) in alternating time intervals of maximum 60 min. Within this time we assumed that the air mass origin does not change considerably. The EF_{INP}, which is the ratio of $INP_{concentrator}$ to INP_{total}, was found to be in the range 1–23 over 27 days representing different air masses. The variation in EF_{INP} due to the concentrator is a function of size (Sioutas et al., 1995), thus suggesting that the sampled air masses contain INPs of different sizes. In addition, the variation in EF_{INP} is also dependent on other specific characteristics of the particles, as for example, the density, shape, and chemistry. In order to calculate ambient INP concentrations from measurements performed by HINC downstream of the concentrator inlet, we used an EF_{INP} of 4 or 17, dependent on the concentration of ambient aerosol particles d >0.5 μm, with a threshold of 0.1/cm^3 (below an EF_{INP} of 4, and above of 17 was applied). This is based on the findings of a correlation between EF_{INP} and the particle concentration in this size range (Spearman's rank correlation coefficient = 0.71, p-value 0.003; see Figure A2 in the appendix), which we believe reflects a change in air mass type.

2.3. Classification of Air Masses

Due to the location of the JFJ, the site is exposed to a variety of air masses and thus aerosol populations, which contribute to the INP population. In this study, four main classes of air mass origin are distinguished: all conditions (all), air masses with significant contributions from the local boundary layer (BLIs), all conditions in the FT (FT_{all}), and background FT conditions ($FT_{background}$), which is FT_{all} but excludes SDEs and marine influenced air masses (Lacher et al., 2017). Although the particles being present during such events are originally emitted from the boundary layer, they undergo long-range transport in the FT, and as such their impact is not limited to a local scale. The differentiation between FT_{all} and $FT_{background}$ is crucial, since the strength and regularity of SDEs and marine events might be variable in the FT, depending on, for example, the distance to source regions. Measurements influenced by local anthropogenic emissions from tourist activities, such as smoking at the JFJ, are excluded for all cases analyzed in this study.

2.3.1. Boundary Layer Injections

In recent years several approaches were determined to identify the influence from local BLI at the JFJ (Griffiths et al., 2014; Henne et al., 2010; Herrmann et al., 2015; Lugauer et al., 1998; Pandey Deolal et al., 2013; Zanis et al., 2007; Zellweger et al., 2003). This is mostly caused by convection of air masses from the regional boundary layer, which can contain increased amounts of e.g., particles emitted from vegetation and soils, as well as from anthropogenic activities. In this study, two measurement-based approaches to determine BLI were used, based on aerosol size distribution properties and trace gas measurements.

The abundance of accumulation mode particles in the FT is naturally very low since no particles of this size are directly formed within the FT (Herrmann et al., 2015). Accumulation mode particles in the FT are thereby only present due to long-range transport in the FT and during BLI from local sources. Hence, increased concentrations are only caused by vertical transport from the boundary layer; therefore, the number concentration of accumulation mode particles can be used to determine BLI. The lower limit of the accumulation mode is often reported to be a diameter between 80 (Kulkarni et al., 2011) and 100 nm (Seinfeld & Pandis, 2016). In this study a diameter of 90 nm is used as a lower limit for the accumulation mode and to identify BLI, as discussed in Herrmann et al. (2015). The number concentration of particles with diameters >90 nm (N90) was obtained from SMPS scans (Herrmann et al., 2015). If the N90 exceeded a threshold of 100/cm^3 in winter and 150/cm^3 in spring/summer (defined as the warm season), respectively, BLI was inferred. These thresholds were chosen according to the findings of Herrmann et al. (2015). They were derived from the aerosol concentration of accumulation mode particles in the background FT, which is nonzero due to long range transport of particles. These findings were based on a six-year time series of size distribution measurements and were supported by Lagrangian backward transport simulations providing the

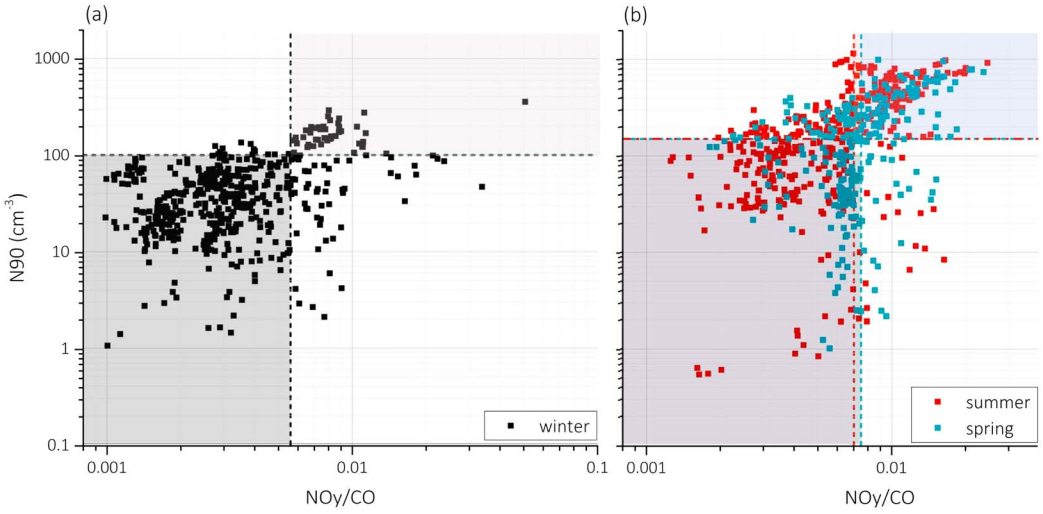

Figure 2. Correlation of N90 with NO_y/CO, data in the dark shaded quadrant represents free troposphere conditions, and light shaded quadrant boundary layer injection. Data appearing in the unshaded quadrants, which indicate disagreement between the two methods, are not taken into account for free troposphere classification; (a) winter measurements with distinction values for N90 = 100/cm^3 and NO_y/CO = 0.0057; (b) spring and summer measurements with distinction values for N90 = 150/cm^3 and NO_y/CO = 0.007 and 0.0069, respectively.

time since air masses' last boundary layer contact. Different thresholds were chosen since particle number concentrations within an air mass originating from the boundary layer follow a seasonal cycle, containing higher concentrations in the warm seasons and lower concentrations in winter. Another common approach to identify BLI in the FT at elevated stations is based on trace gas measurements (Griffiths et al., 2014; Herrmann et al., 2015; Pandey Deolal et al., 2013; Zanis et al., 2007; Zellweger et al., 2003). Total reactive nitrogen (NO_y, as the sum of nitrogen oxide, nitrogen, dioxide and its atmospheric oxidation products) and carbon monoxide (CO) are both emitted from anthropogenic sources, however, with a different atmospheric lifetime on the order of days. While CO is quite constant over this period, NO_y concentrations decrease with increasing residence time in the atmosphere due to wet and dry deposition. Due to this dependence, different NO_y/CO thresholds were chosen, with a NO_y/CO ratio of 0.0057 for winter, 0.0075 for spring, and 0.007 for summer, based on two years of continuous measurements and assessed for different meteorological conditions (Zellweger et al., 2003). A NO_y/CO ratio below the respective threshold is representative of FT conditions. CO was measured with a cavity ringdown spectrometer (Picarro Inc., G2401), and NO_y was measured with a highly sensitive nitrogen monoxide (NO) analyzer, based on chemiluminescence detection (Eco Physics CLD89p) after conversion of NO_y to NO on a heated gold catalyst. Trace gas measurements were taken at a time resolution of 10 min.

In the study by Herrmann et al. (2015) these two identification criteria were evaluated against each other, with a squared correlation coefficient of 99%, which strengthens their applicability to be used as quantitative discrimination criteria for BLI and FT at the JFJ.

In our study, both methods, the N90 and the NO_y/CO ratio, are used to determine if our sampling occurred during FT conditions. Both the N90 and NO_y/CO ratio criteria need to be fulfilled in order to classify an air mass as FT. Only in cases where one criterion is not available (24% of the cases), a sole identification with the available method is applied. A comparison for the two methods is shown in Figure 2 and reveals that the majority of the data as measured in the different seasons fall in the same category for either FT or BLI (74%).

2.3.2. Saharan Dust Events

Events of Saharan dust particles transported to the sampling site are not considered as BLI, since the particles were transported over long distances in the FT and might have been exposed to atmospheric aging processes. SDEs were identified by the single-scattering albedo (SSA) Ångström exponent (Collaud Coen et al., 2004) when the majority of particles are dominated by this particle type. The SSA Ångström exponent was derived for wavelengths of 450, 550, and 700 nm from measurements of the total aerosol scattering coefficients (at three wavelengths) and the absorption coefficients (at seven wavelengths), which were

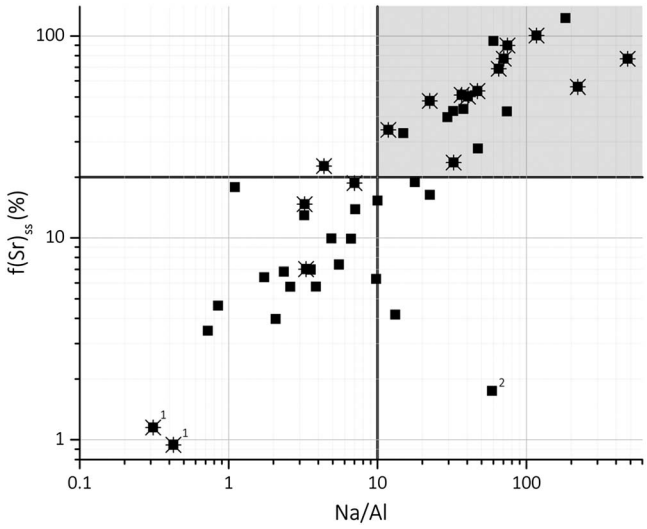

Figure 3. Distribution of ice nucleating particle measurements showing the proportion that are classified as marine events (grey shaded area). Each data points refers to an ice nucleating particle measurements averaged over the sampling time of the cloud water samples; asterisks indicate measurements during free troposphere conditions; the solid horizontal and vertical lines represent the threshold for $f\,(Sr)_{ss}$ and Na/Al (20% and a ratio of 10), respectively, to determine marine influence (see text for details); [1]Saharan dust events; [2]local anthropogenic influence.

measured by an integrating nephelometer (TSI, 3563) and an aethalometer (MAGEE scientific, AE31), respectively, with a time resolution of 1 min. Further information on the procedure can be found in Collaud Coen et al. (2004). The SSA of the normal background aerosol increases with wavelength, which results in a positive SSA Ångström exponent, while a wavelength dependent decrease of the SSA is observed for Saharan dust particles. The resulting negative Ångström exponent is explained by the larger size and different chemical composition and hence different optical properties of the dust particles as compared to the background aerosol.

2.3.3. Marine Events

The influence of air masses originating in the marine boundary layer is also considered to be part of the FT at the JFJ, since the air mass was transported for long distances in the FT. Marine events were determined by the analysis of cloud water samples taken in parallel to the INP measurements, in the presence of clouds. The sampling times thereby depended on the cloud water content, resulting in a nonuniform time resolution of the samples. Comparisons to INP concentrations were done using averages of the latter over the respective sampling period of the cloud water samples. Details are given in Boose, Kanji et al. (2016) and Lacher et al. (2017). Samples were analyzed for 23 different trace metal concentrations, with an inductively coupled plasma mass spectrometer (Agilent, 7500cx) as discussed in Zipori et al. (2012) and Zipori et al. (2015). The marine air mass influence was determined by the fraction of strontium (Sr) coming from sea salt ($f\,(Sr)_{ss}$), which is based on the fact that sodium (Na^+) is found in considerable amounts in sea spray particles, and in cloud water samples, and is always accompanied by Sr if the air mass originates in the marine boundary layer. This results in a constant fraction of Sr to Na^+ of 0.00075 (Turekian, 1968). By comparing the fractions measured in cloud water samples at the JFJ to this constant fraction thus yields an indication of marine influence:

$$f(\mathrm{Sr})_{ss} = \left[\frac{\mathrm{Sr}}{\mathrm{Na^+}}\right]_{ss} \times \left[\frac{\mathrm{Na^+}}{\mathrm{Sr}}\right]_{samp} \quad (1)$$

where $[Sr/Na^+]_{ss}$ is the Sr to Na^+ ratio found in sea salt and $[Na^+/Sr]_{samp}$ is the ratio of Na^+ to Sr found in the cloud samples (Herut et al., 1993). A threshold of >20% was used to identify a considerable influence from air masses originating in the marine boundary layer, which reflects the lower limit of the $f\,(Sr)_{ss}$ representative for marine air from Zipori et al. (2015). By doing so, we take dilution effects into account, which are dominant at the JFJ since it is further away from marine regions, as compared to Zipori et al. (2015). In order to exclude the influence of dust on the sampled air mass, we analyzed the ratio of Na to aluminum (Al) in the cloud water, which is a tracer for mineral dust. A threshold of >10 was chosen to confidently exclude contributions from dust, which is well above the value determined during SDEs at <1. A marine event was only declared when the elemental ratio of Na/Al and the $f\,(Sr)_{ss}$ both fulfill the threshold criteria (Figure 3).

A marine air mass influence as observed by the cloud water sample analysis can last for several hours. Due to the nature of the method the identification of such an event is limited to times when clouds were present at the JFJ. In addition, the sampling procedure is dependent on the liquid water content of the cloud, and as such only 21% of the clouds during the study time have been probed, and only 10% of the total sampling time (in and out of cloud). Therefore, the number of marine air mass events reported here could represent a lower limit of occurrence.

2.4. INP Measurements in the FT

Measurements of INP concentrations at 241–242 K above water saturation in the FT were conducted between 2014 and 2017 at the JFJ, with a focus on wintertime measurements (Boose, Kanji, et al., 2016; Lacher et al., 2017). INP concentrations at 241–242 K ranged from <1/stdL to several tens to hundreds $stdL^{-1}$. Relatively high INP concentrations were observed when the site was influenced by events of marine air mass influence (marine events) and SDEs.

Other INP measurements at different locations in the FT are presented in the following: Airborne sampling of INP concentrations was conducted during the Ice in Clouds Experiment-Layer Clouds (ICE-L; Field et al., 2012) over Wyoming and Colorado, USA, and INP concentrations at 238–243 K ranged from <1 to several tens of INP/stdL. Ground-based measurements were performed during the Ice Nuclei Spectroscopy (INSPECT-1; DeMott, Cziczo, et al., 2003) field campaign at the Storm Peak Laboratory in northwestern Colorado, USA, when INP concentrations at $T > 238$ K were measured in the range from below 10 to above 100/stdL. Due to its location the site is also partly under the influence of local boundary layer air. The ACAPEX (ARM [Atmospheric Radiation Measurement] Cloud Aerosol Precipitation Experiment) field campaign (Ralph et al., 2016) aimed at investigating atmospheric rivers, aerosol sources, and transport processes, which influence cloud and precipitation processes, and research flights were conducted over the ocean and coastal regions over California. The data are a subset of a larger study, which will be published elsewhere. INP sampling during these field campaigns were performed with the Colorado State University (CSU) CFDC (Rogers et al., 2001), which has an uncertainty in temperature and RH_w of ±0.5 K and ±2.4% (Richardson, 2009). During the CALIMA field campaigns (Cloud Affecting particles in Mineral dust from the Sahara; Boose, Sierau, et al., 2016) at the Izaña observatory on Tenerife, Canary Islands (2,373 m), INP concentrations at 241 K were <10/stdL under clean conditions and up to several hundred INP INP/stdL during strong SDEs. INP sampling was conducted with PINC.

In order to compare INP concentrations in the background FT as measured at these distinct locations (see section 3.3), the influence from BLIs, dust, and pollution plumes (e.g., biomass burning) was excluded in all data sets. The measurements during ICE-L were taken in wintertime well above the boundary layer, and due to the airborne sampling method, contributions from the BL were negligible. Influence from BLI during INSPECT-1 was excluded based on particle number concentrations >100 nm, representing the lower limit of accumulation mode particles. Also, for the ACAPEX measurements, accumulation mode particles >90 nm were used for identifying FT conditions. Although the ACAPEX data presented here were filtered for FT, they were not for marine influence, since no increase in INP concentrations, as compared to typical INP concentrations in the FT, was associated with marine influence in this data set. During the CALIMA field campaign, INP sampling representative for the FT was derived from nighttime measurements, when particulate matter (PM10) mass concentrations were <10 μg/stdm^3, and in the absence of SDEs, biomass burning events, and nonrain events.

INP measurements during these studies represent sampling periods between 5 and 30 min.

3. Results

INP concentrations above water saturation were measured at the JFJ between winter 2014 and 2017, resulting in a total of nine field campaigns and 515 hr of INP sampling (Table 1) with ~ 11,000 stdL of ambient air sampled. During the winter in 2014, INPs were sampled with PINC (Boose, Kanji, et al., 2016) and since summer 2014 with HINC (Lacher et al., 2017), which was only available since then on. In Lacher et al. (2017) we compare wintertime field measurements from PINC and HINC and find a good agreement, with INP concentrations in the same range. As such we believe that the two chambers are comparable, given that potential differences between INP measurement techniques can be up to a factor of 5–10. Due to improvements of HINC toward a semiautonomous operation, the effective sampling time of each field campaign, which is the sampling time normalized to the duration of the field campaign, increased since summer 2014. First, the results are presented as a summary over all field campaigns and are separated into air mass origin to obtain conditions of a background FT. Subsequently, INP concentrations during these sampling conditions are separated into single-field campaigns, and seasonal and interannual differences are analyzed. At last, we present a comparison of our results to other measurements in the background FT at different locations in order to assess the variation of INP concentrations in this environment and to provide a global perspective.

3.1. Classification of INP Concentrations

The sampled air masses are distinguished as BLI, FT_{all}, and $FT_{background}$ (the latter being a subset of FT_{all}). FT_{all} also includes SDEs and marine events; however, these are excluded from $FT_{background}$ as described in section 2.3. In 43% of the total sampling time, air masses were influenced by BLI, while 57% were identified as FT_{all}, and 51% as $FT_{background}$ (Table 1). The occurrence of FT_{all} depends on season and is less dominant in spring and summer. This is due to an expansion of the (warmer) boundary layer and also due to the nature of

convective lifting of warm air masses, which results in a higher frequency of BLI. During the time of observation, between 9 and 52% of the sampling time in spring and summer was representative for $FT_{background}$. On the other hand, BLI occurred generally less often in winter, and FT conditions prevailed, with occurrences between 27 and 92%. Our findings are in agreement with Herrmann et al. (2015), who state that FT conditions in winter can occur to above 60% of the time and less than 20% in spring and summer.

During several field campaigns, the JFJ was influenced by air masses containing elevated concentrations of INPs when the station was within the FT. These air masses were identified as SDEs and marine events, and usually lasted for a few hours, and increases in INP concentrations up to 3 orders of magnitude were observed (see Lacher et al., 2017, for a detailed discussion of two such events). The occurrence of SDEs and marine events is given in terms of number of events in Table 1. SDEs were more often observed in winter (4 out of 5 events) as compared to the other seasons, as were marine events (6 out of 12 events). By comparing different years where field campaigns in all three seasons were performed (2015 and 2016), a higher number of SDEs and marine events were observed in 2016 (11 events) compared to 2015 (4 events), indicating considerable year-to-year variability. Our observation of a higher occurrence of SDEs in winter is in contrast to the findings of Collaud Coen et al. (2004), who reported a seasonal trend with a maximum in spring. This maximum is explained by the typical export pathway of Saharan dust in this season (Moulin et al., 1998). Thus, the observed difference in the seasonal occurrence of SDEs at JFJ might be explained by natural annual variabilities. Furthermore, we observed more marine events in winter as compared to the warm season, which is consistent with the findings of Cui et al. (2011). This could be explained by an increased relative contribution of BLIs in spring and summer, which in turn reduces the occurrence of FT conditions and as such leading to a decrease of the observable relative contribution of marine air masses, which are transported in the FT to the JFJ.

As can be seen from Figure 4a (Table A1 in the appendix), when measurements were only taken during FT_{all} conditions, the variability in INP concentrations greatly reduces from an initial interquartile range of 34.9/stdL during all conditions to an interquartile range of 13.1/stdL. Furthermore, the median (mean) INP concentration during FT_{all} conditions reduces to 2.7 (19.7)/stdL, as compared to a median (mean) of 7.2 (52.8)/stdL during all conditions. This reveals that the elevated INP concentrations during all conditions are largely due to BLI, which contain the highest INP concentrations of up to 413.8/stdL (which is still within the 95th percentile and not considered outliers).

During SDEs and marine events, INP concentrations are considerably increased; however, these high INP concentrations only reflect a minority of the total sampling time (2% SDEs, 5% marine events; Table 1). The frequency of these events is important because of the potential role of mineral dust and marine aerosols to the INP population in the background FT (e.g., DeMott, Sassen, et al., 2003; DeMott et al., 2015, 2016; Kamphus et al., 2010; Vergara-Temprado et al., 2017; Wilson et al., 2015). However, no considerable difference between FT_{all} and $FT_{background}$ INP concentrations is found at the JFJ (Figure 4a), which suggests that the $FT_{background}$ is not influenced by the transient nature and occurrence of SDEs and marine events. However, this finding might be different at other locations in the FT, since the occurrence and strengths of these events can be different depending on, for example, the vicinity to the respective sources and respective transport patterns.

A comparison of the n_s for the discussed air mass classifications (see Figure 4b) reveals that there is no considerable difference between BLI, $FT_{background}$, and FT_{all}. The similar n_s values suggest that the differences in INP concentrations reflect the availability of total surface area, which is decreased in the $FT_{background}$. Only during SDEs and marine events higher n_s values are observed indicating that small change in the contribution of these air masses might influence INP concentrations. The comparable n_s values during BLI, FT_{all}, and $FT_{background}$ conditions confirm that the INP concentration is not dominated by the transient increase in INP concentrations during SDEs and marine events. Furthermore, it is possible that aging processes may not affect the ice nucleation ability of ambient particles given that the range of n_s during $FT_{background}$ is similar to that of the BLI as seen in Figure 4. In a study by China et al. (2017), a very small change in the ice nucleation activity between ambient particles was observed, despite differences in the particle chemical composition, source regions, and transport pathways. They concluded that aging did not play a significant role in the ice nucleation activity of ambient particles. We note, however, in our study, that the chemical composition of $FT_{background}$ and BLI aerosol could be very different, and thus, it is not possible to completely exclude aging effects on ice nucleation activity.

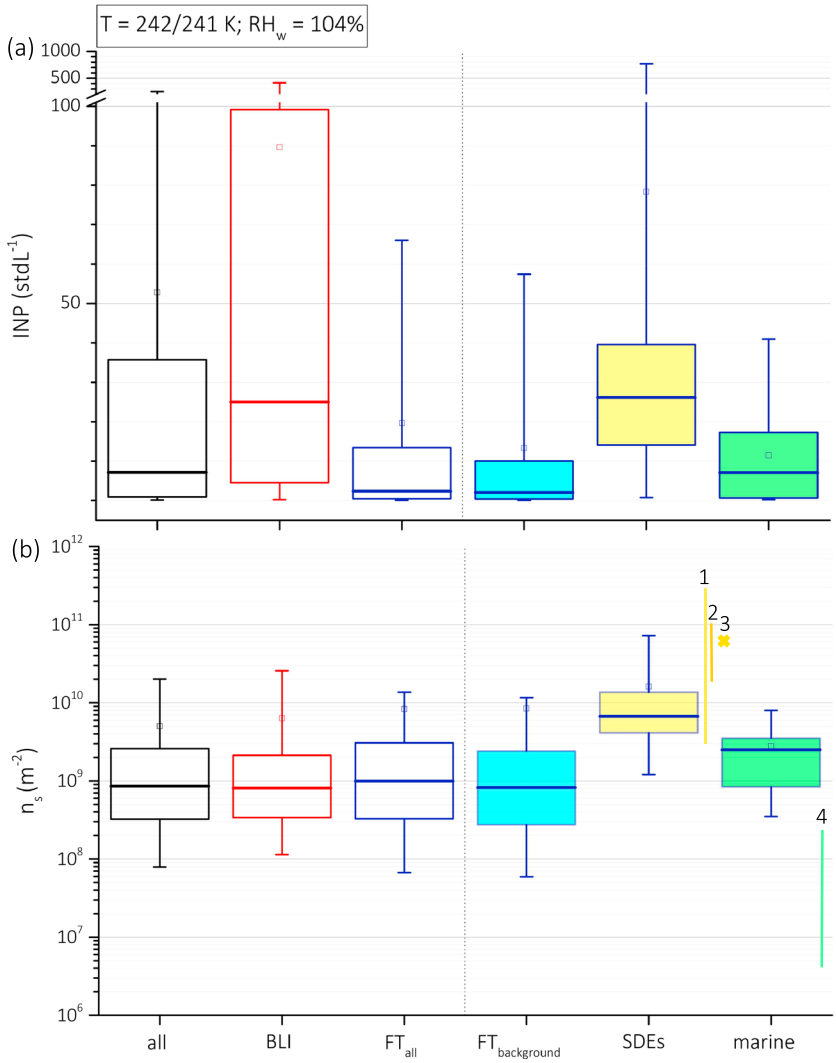

Figure 4. (a) Ice nucleating particle concentrations and (b) n_s as analyzed for the different air mass categories sampled during the field campaigns at the High Altitude Research Station Jungfraujoch between winter 2014 and winter 2017; see text for definition of categories; the filled boxplots are a subgroup of FT_{all}. The thick line and square data point are the median and the mean, respectively; the box represents the interquartile range (25th–75th quartiles); and the whiskers are the 5th and 95th percentiles; 1 refers to range of n_s from laboratory studies on desert dust samples (Connolly et al., 2009; DeMott et al., 2011; Koehler et al., 2010) and 2 to airborne Saharan dust samples measured in the laboratory (Boose, Welti et al., 2016); 3 is based on the parameterization of Niemand et al. (2012); 4 refers to range of n_s from laboratory studies on natural seawater aerosol emission (DeMott et al., 2016).

The range of n_s derived for the SDEs is at the lower end of but still within the range of laboratory studies on desert dust, as depicted in Figure 4b (1, ground collected Saharan dust; Connolly et al., 2009; DeMott et al., 2011; Koehler et al., 2010; 2, airborne Saharan dust Boose, Welti et al., 2016; and 3, ground collected Saharan dust Niemand et al., 2012). In light of numerous laboratory studies showing that coating or exposure of dust particles to atmospheric aging components (e.g., Kanji et al., 2013; Sullivan et al., 2010) can potentially reduce IN activity, it is not surprising that the JFJ SDE n_s is lower, given its long distance to the source region. The reduced n_s for the SDE therefore supports the possibility of aging impacting IN activity, especially when the INP is mineral dust. In addition, Boose, Welti et al. (2016) shows that the n_s from resuspended airborne dust was lower than for surface collected dusts, suggesting that airborne dust indeed has a lower IN activity. As such, it can be expected that the JFJ SDE n_s is not only lower as compared to the surface collected dust from (1) and (3) but also to the airborne collected dust samples from (2), given the longer travel time to the JFJ. However, we acknowledge that the mineralogical composition of the sampled dust particles at the JFJ

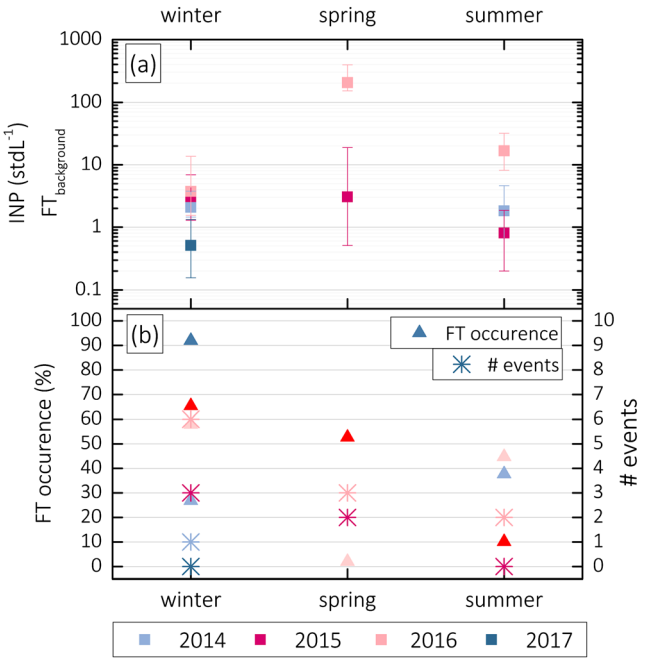

Figure 5. Seasonal and annual distinction of (a) $FT_{background}$ median ice nucleating particle concentrations (squares) and interquartile range (whiskers), measured at T = 242/241 K and RH_w = 104%; (b) the occurrence of $FT_{background}$ conditions relative to the respective field campaign sampling time (triangle) and number of both Saharan dust events and marine events (asterisks).

might be different compared to the dust samples used in the respective laboratory studies and is a caveat to such a comparison and an interpretation for the influence of aging processes. The higher n_s during the marine events at the JFJ as compared to laboratory studies on natural seawater sampled at offshore Californian coast (4; DeMott et al., 2016) might be explained by different factors. First, the air masses sampled during marine influence at the JFJ cannot be claimed to be purely of marine origin, since mixing and entrainment of air masses of different origins would have occurred causing external mixing or internal mixing (aging) during transport of the marine air mass to the JFJ. In addition, the source regions of the marine events at the JFJ were mostly over the Northern and Norwegian Sea (Lacher et al., 2017), which might be quite different in terms of the biological activity as compared to the samples of DeMott et al. (2016). For example, ice active marine species were found to be connected to phytoplankton activity (Knopf et al., 2011; Ladino et al., 2016; McCluskey et al., 2017; Wilson et al., 2015), which is influenced by chlorophyll a concentration, and satellite observations indeed revealed that chlorophyll a concentration are enriched in the Northern latitudes $\gtrsim$40°, as shown in the study by Burrows et al. (2013). Also, Wilson et al. (2015) observed that the onset of freezing for sea surface microlayer samples from Arctic regions occurred at warmer temperatures as compared to samples taken in the Atlantic Ocean, indicating a potential natural variability in the ice nucleation activity of aerosols with different marine sources. To further understand this difference, measurements on the sampled ice crystals during the marine events at the JFJ or more studies on the ice nucleation activity on ocean-emitted aerosols would be desirable.

3.2. Seasonal and Annual Cycle in $FT_{background}$ INP Concentrations

INP concentrations during $FT_{background}$ as measured in separate seasons and years are shown in Figure 5a. The median INP concentrations vary for most field campaigns between 0.5 and 3.7/stdL, and only in the field campaigns of the warm season in 2016, median INP concentrations were above 10 (summer 2016) and 100/stdL (spring 2016). In general, the 2016 field campaigns yielded higher $FT_{background}$ INP concentrations as compared to field campaigns in the same season of different years. For example, not only did the spring and summer measurements in 2016 yield the highest median INP concentration in the respective season but also the highest wintertime INP concentrations were measured in 2016. During the field campaigns in 2016, more SDEs and marine events were observed (Figure 5b), which might explain elevated average INP concentrations. During the winter 2016 measurements, two SDEs and four marine events were identified, and also in spring and summer 2016 more events occurred (three and two marine events, respectively), as compared to the years 2014, 2015, and 2017 (see Table 1). Although $FT_{background}$ excludes identified SDEs and marine events, it is still possible that smaller contributions of particles, which are present during such events, but which do not cause the air mass to fulfill the identification criteria (section 2.3), contribute to the INP population.

In addition, the occurrence of FT conditions in spring 2016 was very low, and as a result the derived $FT_{background}$ INP concentrations in spring 2016 represent only ~2% of the total sampling time in FT conditions. Excluding measurements in this campaign from all measurements conducted between 2014 and 2017 yields only small differences in the overall median (mean) INP concentration of 0.1 (3.2)/stdL, which implies that the spring 2016 $FT_{background}$ does not greatly influence the averages of $FT_{background}$ INP concentrations as presented in Figure 4b.

With the exception of spring and summer 2016, the seasonal averaged INP concentrations of the field campaigns show that $FT_{background}$ INP concentrations are remarkably constant through the three studied seasons (Figure 5a). This is not surprising if one were to consider that the FT is decoupled from direct surface emissions (e.g., Stull, 1988), which excludes influence from seasonally variable boundary layer emissions due to, for example, the phenological season. Only via long-range transport do boundary layer aerosol particles reach the FT. Thus, the aerosol population in the FT is less variable in space and time, as compared to

Table 2
Overview of FT Measurements During CALIMA, INSPECT-1[a], ICE-L and ICE-L CVI[b], and ACAPEX[c]

Name	Time	Longitude (°)	Latitude (°)	Altitude (m)		Location
CALIMA	Summer 2014	−16.500	28.309	2,373	Ground-based	Izaña Atmospheric Observatory, Tenerife
INSPECT-1	Autumn 2001	40.455	106.744	3,220	Ground-based	Storm Peak Laboratory
ICE-L CVI	Winter 2007	41.146	104.802	>2,500	Airborne	Wyoming/Colorado, USA
ICE-L	Winter 2007	41.146	104.802	>2,500	Airborne	Wyoming/Colorado, USA
ACAPEX	Winter 2015	−125.395 to −119.418	36.242 to 40.036	>1,740	Airborne	Californian West Coast/Ocean USA

Note. ACAPEX, ARM (Atmospheric Radiation Measurement) Cloud Aerosol Precipitation Experiment; CALIMA, Cloud Affecting particles in Mineral dust from the Sahara; FT, free troposphere; ICE-L, Ice in Clouds Experiment-Layer Clouds; INSPECT-1, Ice Nuclei Spectroscopy.
[a]DeMott, Cziczo et al. (2003). [b]Same as ICE-L but measurements conducted after a Counterflow Virtual Impactor, hence referring to ice residuals (Eidhammer et al., 2010). [c]Data only reflect an extract of the measurements, which will be the topic of an upcoming study.

boundary layer air, and it is plausible that INP concentrations are also less variable. It should be noted that the measurements presented here are only representative for the given observation periods, which are still limited in time and space. With regard to the higher INP concentrations in spring and summer 2016, more continuous measurements on a monitoring basis are required to understand how frequent such high INP concentrations occur.

3.3. Global Perspective

To compare the presented $FT_{background}$ INP concentrations from JFJ to INP measurements in the FT to those at other locations, measurements from several field campaigns performed with CFDCs were analyzed for similar temperature and RH conditions ($T = 242 \pm 1$ K, immersion freezing). Sampling conditions were determined by excluding BLI, dust, and pollution plumes and influence from biomass burning. An overview of the field campaigns is provided in Table 2 and described in section 2.4. It should be kept in mind that a comparison between INP concentrations at the different locations presented in Figure 6 can also present some variability due to the different instruments used (CSU-CFDC, HINC, and PINC). Intercomparison studies of such instruments have been presented before through laboratory-based campaigns (Hiranuma et al., 2015; Kanji et al., 2011) and have shown in general good agreement given all uncertainties and instrument differences. In light of potential differences expected due to instrument uncertainties, which can be up to a factor of 5–10, the agreement between the concentrations presented in Figure 6 is even more remarkable, suggesting that a relatively constrained INP concentration as shown in Figure 6 is truly a feature of the FT, for the sites considered here.

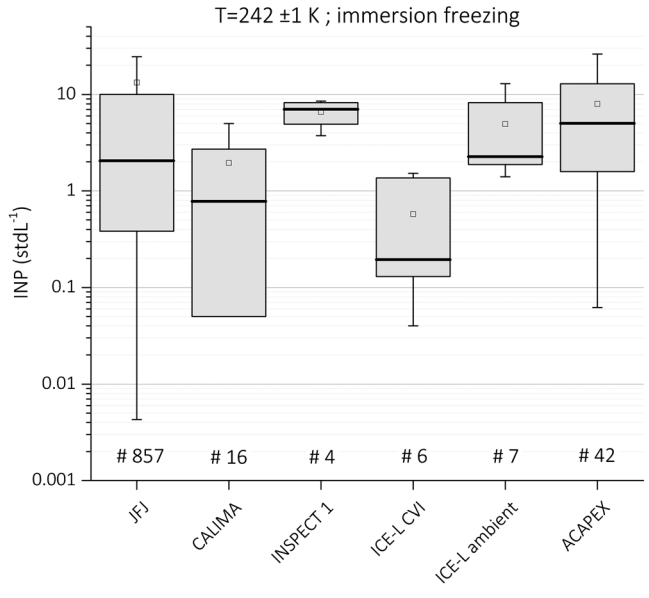

Figure 6. Background free troposphere ice nucleating particle concentrations as measured at the High Altitude Research Station Jungfraujoch (this work), and during Cloud Affecting particles in Mineral dust from the Sahara (CALIMA; Boose, Sierau et al., 2016), Ice Nuclei Spectroscopy (INSPECT-1; DeMott, Cziczo, et al., 2003), Ice in Clouds Experiment-Layer Clouds (ICE-L) and ICE-L CVI (Eidhammer et al., 2010), and ARM (Atmospheric Radiation Measurement) Cloud Aerosol Precipitation Experiment (ACAPEX; see text for more details); the thick line represents the median, the square represents the mean, the box represents the interquartile range, and the whiskers are the 5th and the 95th percentiles.

INP concentrations at the different sampling locations in the background FT do not show a large variation (Figure 6). The median (mean) INP concentrations from the individual campaigns range from 0.2 to 7/stdL (0.6 to 13.3/stdL), and the interquartile range is within 0.05–13/stdL. It is striking that the INP concentrations in the $FT_{background}$ are mostly below 10/stdL for the presented field campaign locations. This suggests that higher variability in INP concentrations as measured at high-altitude stations (e.g., Chou et al., 2011; Richardson et al., 2007) are caused by air masses, which are not strictly representative for $FT_{background}$ but are mixed with, for example, boundary layer, or dusty, or pollution-laden air masses.

Our findings might be used to better constrain INP number concentrations for model use; albeit, here, we present numbers only for ~242 K. Common model parameterizations are based on laboratory studies of a specific type of aerosol particles (e.g., Niemand et al., 2012) and hence follow the seasonal emission and presence of the type of particles in the atmosphere. While a model study by Hande et al. (2015) found that INP number concentrations prescribed by Saharan dust particles are following a seasonal cycle

of the same, our long-term observations suggest that no seasonal or spatial influence on INP concentrations occurs in the FT, thus challenging the need for a parameterization of INP in the FT dependent on a seasonal cycle. Our results are further supported by measurements in different locations in the $FT_{background}$, indicating that a similar behavior can be expected on a global scale.

4. Conclusion

In this paper we present measurements from a total of 9 field campaigns in winter, spring, and summer between 2014 and 2017 at the JFJ, which is located within the FT. Measurements were performed in the immersion freezing mode, in winter 2014 with PINC (Boose, Kanji et al., 2016) at 241 K and RH_w = 103%, and since summer 2014 with HINC (Lacher et al., 2017) at 242 K and RH_w = 104%. The JFJ is generally located within the FT but can be influenced by air mass injections from the local boundary layer. Additionally, Saharan dust and marine particles reach the site via long-range transport and are associated with short-term increases in INP concentration. By excluding influences from boundary layer air, SDEs, and marine events, we determine a background FT INP concentration. During the time of observation, JFJ experienced such conditions for 9–52% of the sampling time in spring and summer and 27–92% in winter. We find that the concentration range of FT INPs at JFJ significantly reduces from an interquartile range of 0.9–35.8/stdL, for all measurements, to an interquartile range of 0.4–10/stdL in the background FT. The finding of an upper bound in the range of 10 INP/stdL (3rd quartile) is supported by the comparison to background FT INP concentrations as measured at different locations (see Figure 6) yielding similar upper bounds in INP concentrations (<13/stdL, 3rd quartile).

A seasonal analysis of median INP concentrations in the background FT shows no strong trend or particular variation. However, INP concentrations were higher in the field campaigns of 2016 as compared to previous years in the respective season, with outlying high concentrations in spring and summer. This is explained by the greatly reduced FT occurrence (14%) during spring and summer 2016 and the increased occurrence of SDEs and marine events in the FT during all three seasons that were sampled. Although these events are excluded from the analysis of a background FT via thresholds, marine and Saharan dust particles might still be present in the background aerosol population, thereby contributing to the observed increases. The presented measurements are first steps in determining a climatology for FT INP concentrations at 242 K. Longer sampling of a systematic monitoring character is needed to clearly identify seasonal patterns.

Appendix A: Uncertainty in Ambient INP Concentrations During Winter 2017

The EF_{INP} has an uncertainty of 14%, which determines that the calculated ambient INP concentrations during winter 2017 has a higher uncertainty of 17%, as compared to the other field campaigns (10%); however, the natural variability in ambient INP concentrations, which can be several orders of magnitude at one temperature (Kanji et al., 2017), outcompetes this instrumental uncertainty. Also, the natural variability of EF_{INP} leads to

Table A1
INP Number Concentrations and n_s at T = 242/241 K and RH_w = 104%[a]

		Mean	1st quartile	Median	3rd quartile	95th percentile[b]
INP concentration ($stdL^{-1}$)	All	52.8	0.9	7.2	35.8	250.9
	BLI	89.6	4.6	25	99.2	413.8
	FT_{all}	19.7	0.4	2.7	13.5	66
	$FT_{background}$	13.3	0.4	2.1	10	57.4
	SDE	78.3	14.1	26.1	39.5	768.8
	Marine event	50.5	0.7	7.6	22.2	187.8
n_s ($10^9/m^2$)	All	1.9	0.17	0.52	1.5	7.1
	BLI	1.1	0.19	0.47	0.96	2.9
	FT_{all}	1.8	0.16	0.6	2	6.9
	$FT_{background}$	1.8	0.16	0.56	1.7	6.9
	SDE	17	3.9	6.9	17	84
	Marine event	2.6	0.61	2.2	3.1	8

Note. BLI, boundary layer injection; FT, free troposphere; INP, ice nucleating particle; RH, relative humidity; SDE, Saharan dust event.
[a]Present in different air mass categories (as visualized in Figure 4). [b]Excluding spring 2016; see text for details.

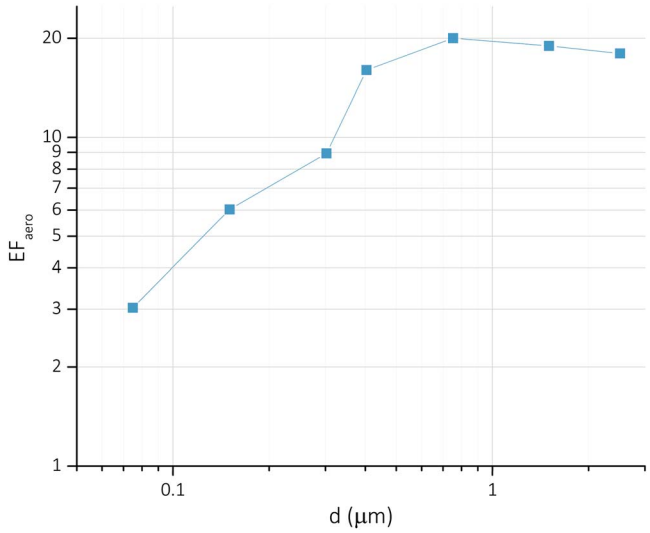

Figure A1. EF_{aero} as function of particle size given in optical diameter; the triangles and squares refer to Scanning Mobility Particle Sizer and OPC measurements, respectively; EF_{aero} represents campaign averages.

elevated uncertainties in the determination of ambient INP concentrations. However, if we apply a constant EF_{INP} as the average over all measured EF_{INP}s during the winter 2017 field campaign, the resulting calculated ambient INP concentration only differs by 0.3/stdL, which is a negligible concentration. By applying a logarithmic fit to the Figure A2 (EF_{INP} as obtained as function of $p > 0.5$ μm,), and using this fit function to calculate INP concentration, the average INP concentration differs only by 0.04/stdL. However, by applying this fit to EF_{INP} as function of particle concentrations $d > 0.5$ μm, the 1-sigma confidence interval reveals that uncertainties of up to a factor of 5 might be possible. This would result in a variation in INP concentrations of 0.5–13.2/stdL for the winter 2017 measurements, which is within the natural variability of the field measurements.

The presented EF_{aero} and EF_{INP} are thereby explicitly representative of air masses arriving at the JFJ from the main source regions (Central Europe, Mediterranean Sea, Atlantic Ocean, North Africa, and the Saharan Desert; Figure A4). Enrichment factors for other sampling locations might be different and would need to be determined separately.

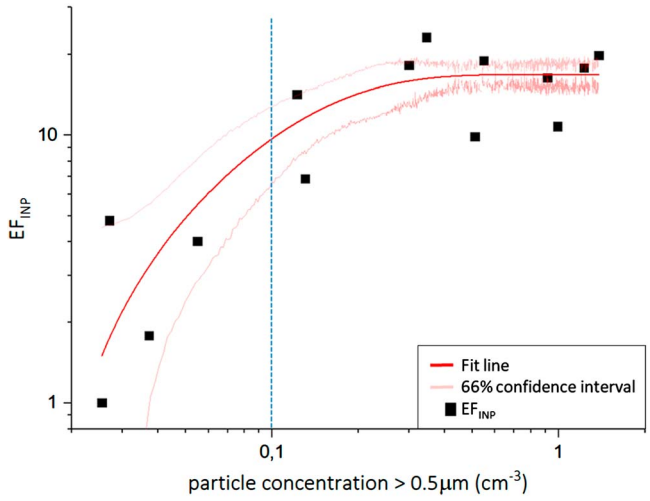

Figure A2. EF_{INP} as function of particle concentrations $d > 0.5$ μm; each EF_{INP} refers to an ice nucleating particle sampling over 40 min (20-min measurement each at the total inlet and the concentrator inlet). The dashed line refers to the threshold ($0.1/cm^3$ for a particle concentration $d > 0.5$ μm) used to derive at the respective EF_{INP}. The red line is the logarithmic fit to the data, and the light red lines represent the 1-sigma confidence interval. The red line is the logarithmic fit to the data, and the shaded area is the 1-sigma confidence interval.

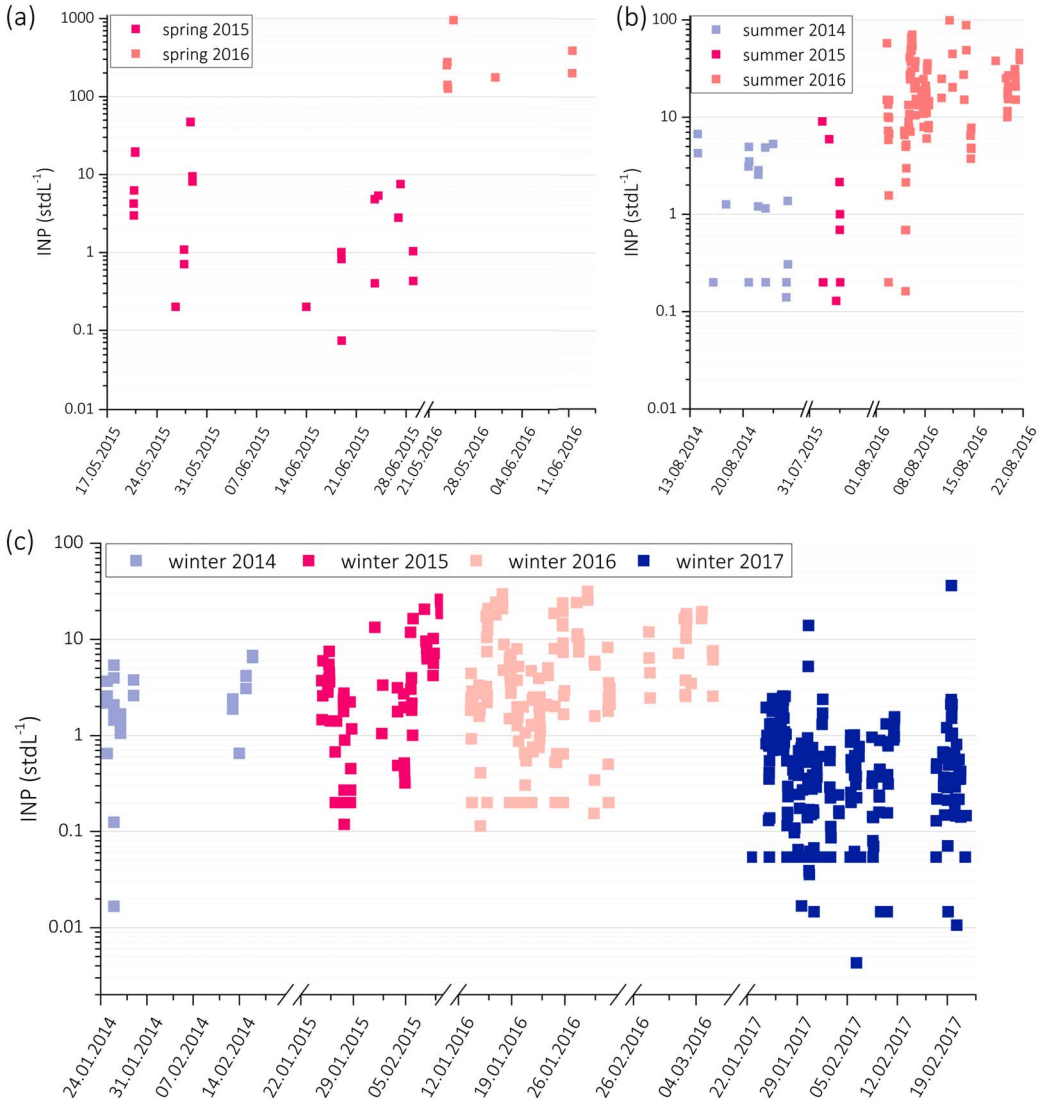

Figure A3. Timeline of $FT_{background}$ ice nucleating particle concentrations measured at T = 241/242 K and RH_w = 104% in the respective field campaigns in (a) spring, (b) summer, and (c) winter; time interval represents one week.

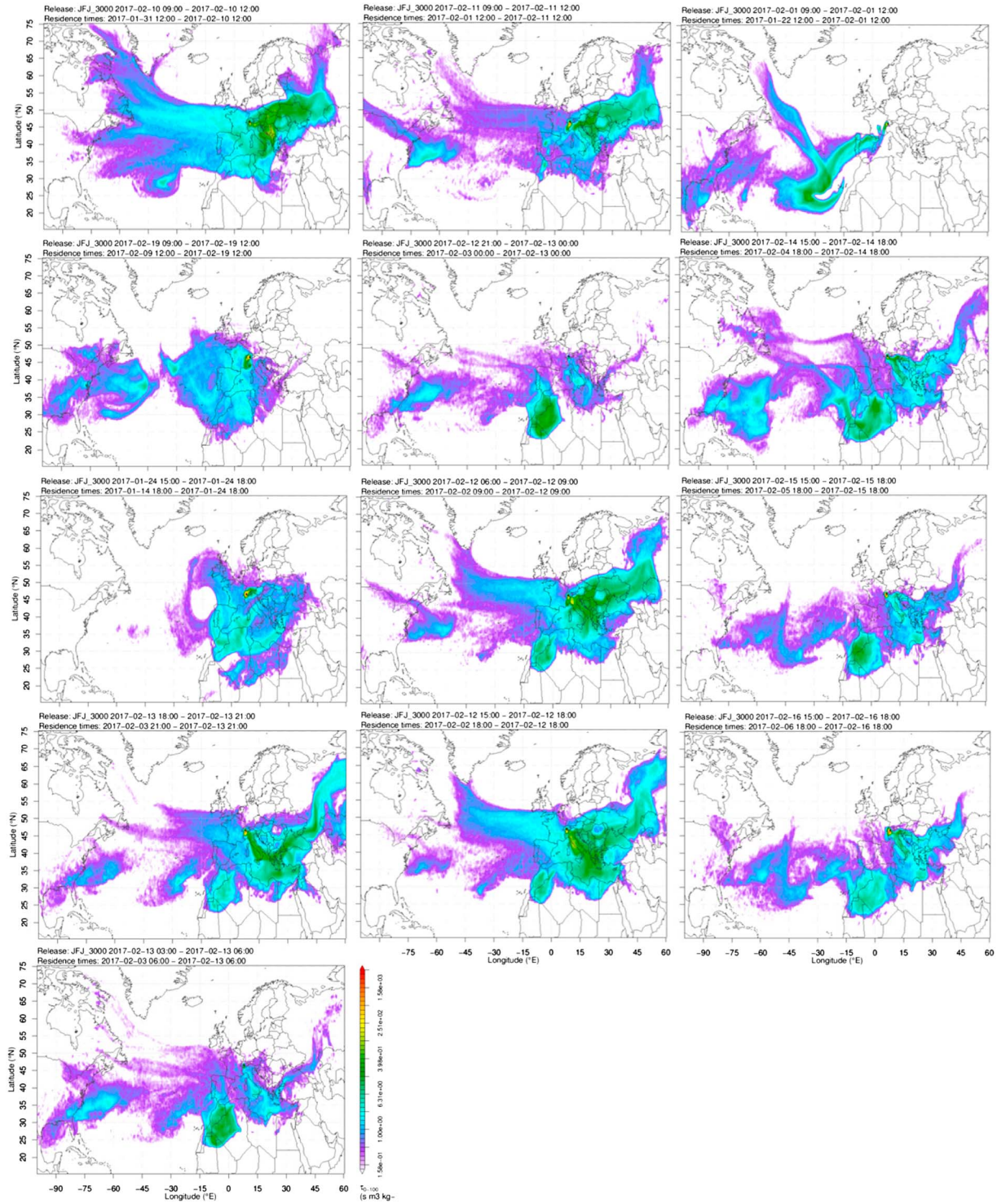

Figure A4. Source emission sensitivities derived from FLEXPART (products browser at EMPA: https://lagrange.empa.ch/FLEXPART_browser/; Pandey Deolal et al., 2014; Stohl et al., 2005; Sturm et al., 2013) for aerosol particles, which were sampled during measurements of EF_{INP}.

Author Contributions

L. L. wrote the manuscript, with contributions from Z. A. K. Z. A. K. and U. L. conceived the field study. Z. A. K. and L. L. designed the laboratory experiments. Field measurements were designed by L. L. , Y. B., and Z. A. K. L. L. conducted all INP measurements and analyzed all INP data. L. L., Z. A. K., and U. L. interpreted the INP data. P. D. and Y. B. contributed data and discussion on FT INP concentrations. E. L. and K. S. contributed data on FT INP concentrations. A. Z. conducted part of the cloud water sampling and analyzed and interpreted the data. E. H. contributed data on size distributions. N. B. contributed data on absorption characteristics. M. S. contributed data on trace gases. E. G. operated the PAPC in winter 2017 JPDA, and E. G. provided PAPC size-dependent concentration factors and interpreted the PAPC data. Z. A. K. oversaw the overall project.

Acknowledgments
Data represented in the figures and analyses are available online at DOI 10.3929/ethz-b-000256801. This research was funded by the Global Atmospheric Watch, Switzerland (MeteoSwiss GAW-CH+ 2014-2017). For the opportunity and support to perform the field campaigns, we thank the International Foundation High Altitude Research Station Jungfraujoch and Gornergrat (HFJG), with a special thanks to the custodians Maria and Urs Otz, Joan and Martin Fischer, and Susanne and Felix Seiler. We thank MeteoSwiss for providing meteorological data. Y. Boose and U. Lohmann acknowledge funding from the European Union's Seventh Framework Programme (FP7/2007-2013) under grant agreement no. 603445 (BACCHUS). Trace gases measured at JFJ are part of the Swiss National Air Pollution Monitoring Network, which is jointly run by EMPA and the Swiss Federal Office for the Environment. This project has also received financial support from the ACTRIS research infrastructure funded by the European Union (H2020-INFRAIA-2014-2015; grant agreement no. 654109) and the Swiss State Secretariat for Education, Research and Innovation (SERI) (contract number 15.0159-1). The opinions expressed and arguments employed herein do not necessarily reflect the official views of the Swiss Government. INSPECT and ICE-L data from the Colorado State University (CSU) CFDC were derived from archived data under support of the grant NSF AGS1358495. CSU CFDC data from the ACAPEX project measurements were supported by the Office of Biological and Environmental Research of the U.S. Department of Energy (as part of the Atmospheric Radiation Measurement Climate Research Facility) under Battelle Memorial Institute (Pacific Northwest National Laboratory) contract 240627, further analyzed under support of the DOE Atmospheric Systems Research program award DE-SC0014354. We acknowledge James Atkinson, Robert David, Anina Gilgen, Fabian Mahrt, Nadine Borduas, and Marco Zanatta for useful discussions. For technical support we would like to thank Hannes Wydler, whose expertise greatly helped to improve the instrument. We acknowledge Philippe Demougin for proofreading the manuscript.

References

Ansmann, A., Tesche, M., Althausen, D., Müller, D., Seifert, P., Freudenthaler, V., et al. (2008). Influence of Saharan dust on cloud glaciation in southern Morocco during the Saharan Mineral Dust Experiment. *Journal of Geophysical Research*, *113*, D04210. https://doi.org/10.1029/2007JD008785

Appenzeller, C., Begert, M., Zenklusen, E., & Scherrer, S. C. (2008). Monitoring climate at Jungfraujoch in the high Swiss Alpine region. *Science of the Total Environment*, *391*(2–3), 262–268. https://doi.org/10.1016/j.scitotenv.2007.10.005

Ardon-Dryer, K., & Levin, Z. (2014). Ground-based measurements of immersion freezing in the eastern Mediterranean. *Atmospheric Chemistry and Physics*, *14*(10), 5217–5231. https://doi.org/10.5194/acp-14-5217-2014

Baltensperger, U., Gäggeler, H. W., Jost, D. T. A. L., Schwikowski, M., & Weingartner, E. (1997). Aerosol climatology at the high-alpine site Jungfraujoch, Switzerland. *Journal of Geophysical Research*, *102*, 19,707–19,715. https://doi.org/10.1029/97JD00928

Bigg, E. K. (1967). Cross sections of ice nucleus concentrations at altitude over long paths. *Journal of the Atmospheric Sciences*, *24*(2), 226–229. https://doi.org/10.1175/1520-0469(1967)024<0226:CSOINC>2.0.CO;2

Bingemer, H., Klein, H., Ebert, M., Haunold, W., Bundke, U., Herrmann, T., et al. (2012). Atmospheric ice nuclei in the Eyjafjallajökull volcanic ash plume. *Atmospheric Chemistry and Physics*, *12*(2), 857–867. https://doi.org/10.5194/acp-12-857-2012

Boose, Y., Kanji, Z. A., Kohn, M., Sierau, B., Zipori, A., Crawford, I., et al. (2016). Ice nucleating particle measurements at 241 K during winter months at 3580 m MSL in the Swiss Alps. *Journal of the Atmospheric Sciences*, *73*(5), 2203–2228. https://doi.org/10.1175/JAS-D-15-0236.1

Boose, Y., Sierau, B., Garcia, M. I., Rodriguez, S., Alastuey, A., Linke, C., et al. (2016). Ice nucleating particles in the Saharan air layer. *Atmospheric Chemistry and Physics*, *16*(14), 9067–9087. https://doi.org/10.5194/acp-16-9067-2016

Boose, Y., Welti, A., Atkinson, J., Ramelli, F., Danielczok, A., Bingemer, H. G., et al. (2016). Heterogeneous ice nucleation on dust particles sourced from nine~deserts worldwide—Part 1: Immersion freezing. *Atmospheric Chemistry and Physics*, *16*(23), 15,075–15,095. https://doi.org/10.5194/acp-16-15075-2016

Boucher, O., et al. (2013). Clouds and aerosols. In T. F. Stocker, D. Qin, G.-K. Plattner, M. Tignor, S. K. Allen, J. Boschung, et al. (Eds.), *Climate change 2013: The physical science basis. Contribution of working group I to the fifth assessment report of the Intergovernmental Panel on Climate Change* (pp. 571–658). Cambridge, United Kingdom and New York, NY: Cambridge University Press. https://doi.org/10.1017/CBO9781107415324.016

Bühl, J., Seifert, P., Myagkov, A., & Ansmann, A. (2016). Measuring ice- and liquid-water properties in mixed-phase cloud layers at the Leipzig Cloudnet station. *Atmospheric Chemistry and Physics*, *16*(16), 10,609–10,620. https://doi.org/10.5194/acp-16-10609-2016

Bukowiecki, N., Weingartner, E., Gysel, M., Collaud Coen, M., Zieger, P., Herrmann, E., et al. (2016). A review of more than 20 years of aerosol observation at the High Altitude Research Station Jungfraujoch, Switzerland (3580 m asl). *Aerosol and Air Quality Research*, *16*(3), 764–788. https://doi.org/10.4209/aaqr.2015.05.0305

Burrows, S. M., Hoose, C., Pöschl, U., & Lawrence, M. G. (2013). Ice nuclei in marine air: biogenic particles or dust? *Atmospheric Chemistry and Physics*, *13*(1), 245–267. https://doi.org/10.5194/acp-13-245-2013

China, S., Alpert, P. A., Zhang, B., Schum, S., Dzepina, K., Wright, K., et al. (2017). Ice cloud formation potential by free tropospheric particles from long-range transport over the northern Atlantic Ocean. *Journal of Geophysical Research: Atmospheres*, *122*, 3065–3079. https://doi.org/10.1002/2016JD025817

Chou, C., Stetzer, O., Weingartner, E., Juranyi, Z., Kanji, Z. A., & Lohmann, U. (2011). Ice nuclei properties within a Sahara dust event at the Jungfraujoch in the Swiss Alps. *Atmospheric Chemistry and Physics*, *11*(10), 4725–4738. https://doi.org/10.5194/acp-11-4725-2011

Collaud Coen, M., Weingartner, E., Furger, M., Nyeki, S., Prévôt, A. S. H., Steinbacher, M., & Baltensperger, U. (2011). Aerosol climatology and planetary boundary influence at the Jungfraujoch analyzed by synoptic weather types. *Atmospheric Chemistry and Physics*, *11*(12), 5931–5944. https://doi.org/10.5194/acp-11-5931-2011

Collaud Coen, M., Weingartner, E., Schaub, D., Hueglin, C., Corrigan, C., Henning, S., et al. (2004). Saharan dust events at the Jungfraujoch: Detection by wavelength dependence of the single scattering albedo and first climatology analysis. *Atmospheric Chemistry and Physics*, *4*(11/12), 2465–2480. https://doi.org/10.5194/acp-4-2465-2004

Conen, F., Morris, C. E., Leifeld, J., Yakutin, M. V., & Alewell, C. (2011). Biological residues define the ice nucleation properties of soil dust. *Atmospheric Chemistry and Physics*, *11*(18), 9643–9648. https://doi.org/10.5194/acp-11-9643-2011

Conen, F., Rodríguez, S., Hüglin, C., Henne, S., Herrmann, E., Bukowiecki, N., & Alewell, C. (2015). Atmospheric ice nuclei at the high-altitude observatory Jungfraujoch, Switzerland. *Tellus B*, *67*(0), 1. https://doi.org/10.3402/tellusb.v67.25014

Conen, F., Stopelli, E., & Zimmermann, L. (2016). Clues that decaying leaves enrich Arctic air with ice nucleating particles. *Atmospheric Environment*, *129*(Supplement C), 91–94. https://doi.org/10.1016/j.atmosenv.2016.01.027

Connolly, P. J., Möhler, O., Field, P. R., Saathoff, H., Burgess, R., Choularton, T., & Gallagher, M. (2009). Studies of heterogeneous freezing by three different desert dust samples. *Atmospheric Chemistry and Physics*, *9*(8), 2805–2824. https://doi.org/10.5194/acp-9-2805-2009

Cui, J., Pandey Deolal, S., Sprenger, M., Henne, S., Staehelin, J., Steinbacher, M., & Nédélec, P. (2011). Free tropospheric ozone changes over Europe as observed at Jungfraujoch (1990–2008): An analysis based on backward trajectories. *Journal of Geophysical Research*, *116*, D10304. https://doi.org/10.1029/2010JD015154

de Boer, G., Morrison, H., Shupe, M. D., & Hildner, R. (2011). Evidence of liquid dependent ice nucleation in high-latitude stratiform clouds from surface remote sensors. *Geophysical Research Letters*, *38*, L01803. https://doi.org/10.1029/2010GL046016

DeMott, P. J., Cziczo, D. J., Prenni, A. J., Murphy, D. M., Kreidenweis, S. M., Thomson, D. S., et al. (2003). Measurements of the concentration and composition of nuclei for cirrus formation. *Proceedings of the National Academy of Sciences*, *100*(25), 14,655–14,660. https://doi.org/10.1073/pnas.2532677100

DeMott, P. J., Hill, T. C. J., McCluskey, C. S., Prather, K. A., Collins, D. B., Sullivan, R. C., et al. (2016). Sea spray aerosol as a unique source of ice nucleating particles. *Proceedings of the National Academy of Sciences*, *113*(21), 5797–5803. https://doi.org/10.1073/pnas.1514034112

DeMott, P. J., Möhler, O., Stetzer, O., Vali, G., Levin, Z., Petters, M. D., et al. (2011). Resurgence in ice nuclei measurement research. *Bulletin of the American Meteorological Society*, *92*(12), 1623–1635. https://doi.org/10.1175/BAMS-D-10-3119.1

DeMott, P. J., Prenni, A. J., Liu, X., Kreidenweis, S. M., Petters, M. D. A. T., Richardson, C. H. M. S., et al. (2010). Predicting global atmospheric ice nuclei distributions and their impacts on climate. *Proceedings of the National Academy of Sciences*, *107*(25), 11,217–11,222. https://doi.org/10.1073/pnas.0910818107

DeMott, P. J., Prenni, A. J., McMeeking, G. R., Sullivan, R. C., Petters, M. D., Tobo, Y., et al. (2015). Integrating laboratory and field data to quantify the immersion freezing ice nucleation activity of mineral dust particles. *Atmospheric Chemistry and Physics*, *15*(1), 393–409. https://doi.org/10.5194/acp-15-393-2015

DeMott, P. J., Sassen, K., Poellot, M. R., Baumgardner, D., Rogers, D. C., Brooks, S. D., et al. (2003). African dust aerosols as atmospheric ice nuclei. *Geophysical Research Letters*, *30*(14), 1732. https://doi.org/10.1029/2003GL017410

Eidhammer, T., DeMott, P. J., Prenni, A. J., Petters, M. D., Twohy, C. H., Rogers, D. C., et al. (2010). Ice initiation by aerosol particles: Measured and predicted ice nuclei concentrations versus measured ice crystal concentrations in an orographic wave cloud. *Journal of the Atmospheric Sciences*, *67*(8), 2417–2436. https://doi.org/10.1175/2010jas3266.1

Field, P. R., Heymsfield, A. J., Shipway, B. J., DeMott, P. J., Pratt, K. A., Rogers, D. C., et al. (2012). Ice in clouds experiment–layer clouds. Part II: Testing characteristics of heterogeneous ice formation in lee wave clouds. *Journal of the Atmospheric Sciences*, *69*(3), 1066–1079. https://doi.org/10.1175/jas-d-11-026.1

Griffiths, A. D., Conen, F., Weingartner, E., Zimmermann, L., Chambers, S. D., Williams, A. G., & Steinbacher, M. (2014). Surface-to-mountaintop transport characterised by radon observations at the Jungfraujoch. *Atmospheric Chemistry and Physics*, *14*(23), 12,763–12,779. https://doi.org/10.5194/acp-14-12763-2014

Griffiths, A. D., Parkes, S. D., Chambers, S. D., McCabe, M. F., & Williams, A. G. (2013). Improved mixing height monitoring through a combination of lidar and radon measurements. *Atmospheric Measurement Techniques*, *6*(2), 207–218. https://doi.org/10.5194/amt-6-207-2013

Hande, L. B., Engler, C., Hoose, C., & Tegen, I. (2015). Seasonal variability of Saharan desert dust and ice nucleating particles over Europe. *Atmospheric Chemistry and Physics*, *15*(8), 4389–4397. https://doi.org/10.5194/acp-15-4389-2015

Henne, S., Brunner, D., Folini, D., Solberg, S., Klausen, J., & Buchmann, B. (2010). Assessment of parameters describing representativeness of air quality in-situ measurement sites. *Atmospheric Chemistry and Physics*, *10*(8), 3561–3581. https://doi.org/10.5194/acp-10-3561-2010

Herrmann, E., Weingartner, E., Henne, S., Vuilleumier, L., Bukowiecki, N., Steinbacher, M., et al. (2015). Analysis of long-term aerosol size distribution data from Jungfraujoch with emphasis on free tropospheric conditions, cloud influence, and air mass transport. *Journal of Geophysical Research: Atmospheres*, *120*, 9459–9480. https://doi.org/10.1002/2015JD023660

Herut, B., Starinsky, A., & Katz, A. (1993). Strontium in rainwater from Israel: Sources, isotopes and chemistry. *Earth and Planetary Science Letters*, *120*(1-2), 77–84. https://doi.org/10.1016/0012-821X(93)90024-4

Hiranuma, N., Augustin-Bauditz, S., Bingemer, H., Budke, C., Curtius, J., Danielczok, A., et al. (2015). A comprehensive laboratory study on the immersion freezing behavior of illite NX particles: A comparison of 17 ice nucleation measurement techniques. *Atmospheric Chemistry and Physics*, *15*(5), 2489–2518. https://doi.org/10.5194/acp-15-2489-2015

Hoose, C., Lohmann, U., Bennartz, R., Croft, B., & Lesins, G. (2008). Global simulations of aerosol processing in clouds. *Atmospheric Chemistry and Physics*, *8*(23), 6939–6963.

Hoose, C., & Möhler, O. (2012). Heterogeneous ice nucleation on atmospheric aerosols: A review of results from laboratory experiments. *Atmospheric Chemistry and Physics*, *12*(20), 9817–9854. https://doi.org/10.5194/acp-12-9817-2012

Kamphus, M., Ettner-Mahl, M., Klimach, T., Drewnick, F., Keller, L., Cziczo, D. J., et al. (2010). Chemical composition of ambient aerosol, ice residues and cloud droplet residues in mixed-phase clouds: Single particle analysis during the Cloud and Aerosol Characterization Experiment (CLACE 6). *Atmospheric Chemistry and Physics*, *10*(16), 8077–8095. https://doi.org/10.5194/acp-10-8077-2010

Kanji, Z. A., DeMott, P. J., Möhler, O., & Abbatt, J. P. D. (2011). Results from the University of Toronto Continuous Flow Diffusion Chamber at ICIS 2007: Instrument intercomparison and ice onsets for different aerosol types. *Atmospheric Chemistry and Physics*, *11*(1), 31–41. https://doi.org/10.5194/acp-11-31-2011

Kanji, Z. A., Ladino, L. A., Wex, H., Boose, Y., Burkert-Kohn, M., Cziczo, D. J., & Krämer, M. (2017). Overview of ice nucleating particles. *Meteorological Monographs*, *58*, 1.1–1.33. https://doi.org/10.1175/amsmonographs-d-16-0006.1

Kanji, Z. A., Welti, A., Chou, C., Stetzer, O., & Lohmann, U. (2013). Laboratory studies of immersion and deposition mode ice nucleation of ozone aged mineral dust particles. *Atmospheric Chemistry and Physics*, *13*(17), 9097–9118. https://doi.org/10.5194/acp-13-9097-2013

Knopf, D. A., Alpert, P. A., Wang, B., & Aller, J. Y. (2011). Stimulation of ice nucleation by marine diatoms. *Nature Geoscience*, *4*(2), 88–90. https://doi.org/10.1038/NGEO1037

Knopf, D. A., Alpert, P. A., Wang, B., O'Brien, R. E., Kelly, S. T., Laskin, A., et al. (2014). Microspectroscopic imaging and characterization of individually identified ice nucleating particles from a case field study. *Journal of Geophysical Research: Atmospheres*, *119*, 10,365–10,381. https://doi.org/10.1002/2014JD021866

Koehler, K. A., Kreidenweis, S. M., DeMott, P. J., Petters, M. D., Prenni, A. J., & Möhler, O. (2010). Laboratory investigations of the impact of mineral dust aerosol on cold cloud formation. *Atmospheric Chemistry and Physics*, *10*(23), 11,955–11,968. https://doi.org/10.5194/acp-10-11955-2010

Korolev, A., McFarquhar, G., Field, P. R., Franklin, C., Lawson, P., Wang, Z., et al. (2017). Mixed-phase clouds: Progress and challenges. *Meteorological Monographs*, *58*, 5.1–5.50. https://doi.org/10.1175/amsmonographs-d-17-0001.1

Kulkarni, P., Baron, P. A., & Willeke, K. (2011). *Aerosol measurement: principles, techniques, and applications*. Hoboken, NJ: John Wiley. https://doi.org/10.1002/9781118001684

Lacher, L., Lohmann, U., Boose, Y., Zipori, A., Herrmann, E., Bukowiecki, N., et al. (2017). The Horizontal Ice Nucleation Chamber (HINC): INP measurements at conditions relevant for mixed-phase clouds at the High Altitude Research Station Jungfraujoch. *Atmospheric Chemistry and Physics*, *17*(24), 15,199–15,224. https://doi.org/10.5194/acp-17-15199-2017

Ladino, L. A., Yakobi-Hancock, J. D., Kilthau, W. P., Mason, R. H., Si, M., Li, J., et al. (2016). Addressing the ice nucleating abilities of marine aerosol: A combination of deposition mode laboratory and field measurements. *Atmospheric Environment*, *132*, 1–10. https://doi.org/10.1016/j.atmosenv.2016.02.028

Ladino Moreno, L., Stetzer, O., & Lohmann, U. (2013). Contact freezing: A review of experimental studies. *Atmospheric Chemistry and Physics*, *13*(19), 9745–9769. https://doi.org/10.5194/acp-13-9745-2013

Lau, K. M., & Wu, H. T. (2003). Warm rain processes over tropical oceans and climate implications. *Geophysical Research Letters*, *30*(24), 2290. https://doi.org/10.1029/2003GL018567

Lohmann, U. (2017). Anthropogenic aerosol influences on mixed-phase clouds. *Current Climate Change Reports*, *3*(1), 32–44. https://doi.org/10.1007/s40641-017-0059-9

Lohmann, U., & Feichter, J. (2005). Global indirect aerosol effects: A review. *Atmospheric Chemistry and Physics*, *5*(3), 715–737. https://doi.org/10.5194/acp-5-715-2005

Lugauer, M., Baltensperger, U., Furger, M., Gäggeler, H. W., Jost, D. T., Schwikowski, M., & Wanner, H. (1998). Aerosol transport to the high Alpine sites Jungfraujoch (3454 m a.s.l.) and Colle Gnifetti (4452 m a.s.l.). *Tellus B*, *50*(1), 76–92. https://doi.org/10.1034/j.1600-0889.1998.00006.x

Mason, R. H., Chou, C., McCluskey, C. S., Levin, E. J. T., Schiller, C. L., Hill, T. C. J., et al. (2015). The micro-orifice uniform deposit impactor–droplet freezing technique (MOUDI-DFT) for measuring concentrations of ice nucleating particles as a function of size: Improvements and initial validation. *Atmospheric Measurement Techniques*, *8*(6), 2449–2462. https://doi.org/10.5194/amt-8-2449-2015

Mason, R. H., Si, M., Li, J., Chou, C., Dickie, R., Toom-Sauntry, D., et al. (2015). Ice nucleating particles at a coastal marine boundary layer site: Correlations with aerosol type and meteorological conditions. *Atmospheric Chemistry and Physics*, *15*(21), 12,547–12,566. https://doi.org/10.5194/acp-15-12547-2015

McCluskey, C. S., Hill, T. C. J., Malfatti, F., Sultana, C. M., Lee, C., Santander, M. V., et al. (2017). A dynamic link between ice nucleating particles released in nascent sea spray aerosol and oceanic biological activity during two Mesocosm experiments. *Journal of the Atmospheric Sciences*, *74*(1), 151–166. https://doi.org/10.1175/jas-d-16-0087.1

Moulin, C., Lambert, C. E., Dayan, U., Masson, V., Ramonet, M., Bousquet, P., et al. (1998). Satellite climatology of African dust transport in the Mediterranean atmosphere. *Journal of Geophysical Research*, *103*(D11), 13,137–13,144. https://doi.org/10.1029/98JD00171

Mülmenstädt, J., Sourdeval, O., Delanoë, J., & Quaas, J. (2015). Frequency of occurrence of rain from liquid-, mixed-, and ice-phase clouds derived from A-Train satellite retrievals. *Geophysical Research Letters*, *42*, 6502–6509. https://doi.org/10.1002/2015GL064604

Nagare, B., Marcolli, C., Welti, A., Stetzer, O., & Lohmann, U. (2016). Comparing contact and immersion freezing from Continuous Flow Diffusion Chambers. *Atmospheric Chemistry and Physics*, *16*(14), 8899–8914. https://doi.org/10.5194/acp-16-8899-2016

Niemand, M., Möhler, O., Vogel, B., Vogel, H., Hoose, C., Connolly, P., et al. (2012). A particle-surface-area-based parameterization of immersion freezing on desert dust particles. *Journal of the Atmospheric Sciences*, *69*(10), 3077–3092. https://doi.org/10.1175/JAS-D-11-0249.1

Nyeki, S., Li, F., Weingartner, E., Streit, N., Colbeck, I., Gäggeler, H. W., & Baltensperger, U. (1998). The background aerosol size distribution in the free troposphere: An analysis of the annual cycle at a high-alpine site. *Journal of Geophysical Research*, *103*(D24), 31,749–31,761. https://doi.org/10.1029/1998JD200029

Pandey Deolal, S., Henne, S., Ries, L., Gilge, S., Weers, U., Steinbacher, M., et al. (2014). Analysis of elevated springtime levels of Peroxyacetyl nitrate (PAN) at the high Alpine research sites Jungfraujoch and Zugspitze. *Atmospheric Chemistry and Physics*, *14*, 12,553–12,571.

Pandey Deolal, S., Staehelin, J., Brunner, D., Cui, J., Steinbacher, M., Zellweger, C., et al. (2013). Transport of PAN and NOy from different source regions to the Swiss high alpine site Jungfraujoch. *Atmospheric Environment*, *64*, 103–115. https://doi.org/10.1016/j.atmosenv.2012.08.021

Pöschl, U. (2005). Atmospheric aerosols: Composition, transformation, climate and health effects. *Angewandte Chemie, International Edition*, *44*(46), 7520–7540. https://doi.org/10.1002/anie.200501122

Prenni, A., DeMott, P., Rogers, D., Kreidenweis, S. M., McFarquhar, G. M., Zhang, G., & Poellot, M. R. (2009). Ice nuclei characteristics from M-PACE and their relation to ice formation in clouds. *Tellus B*, *61*(2), 436–448. https://doi.org/10.1111/j.1600-0889.2009.00415.x

Ralph, F. M., Prather, K. A., Cayan, D., Spackman, J. R., DeMott, P., Dettinger, M., et al. (2016). CalWater field studies designed to quantify the roles of atmospheric rivers and aerosols in modulating U.S. West Coast Precipitation in a Changing Climate. *Bulletin of the American Meteorological Society*, *97*(7), 1209–1228. https://doi.org/10.1175/bams-d-14-00043.1

Richardson, M. S. (2009). *Making real time measurements of ice nuclei concentrations at upper tropospheric temperatures: Extending the capabilities of the continuous flow diffusion chamber* (p. 268). Fort Collins: Colorado State University.

Richardson, M. S., Demott, P. J., Kreidenweis, S. M., Cziczo, D. J., Dunlea, E. J., Jimenez, J. L., et al. (2007). Measurements of heterogeneous ice nuclei in the western United States in springtime and their relation to aerosol characteristics. *Journal of Geophysical Research*, *112*, D02209. https://doi.org/10.1029/2006JD007500

Rogers, D. C. (1988). Development of a continuous flow thermal gradient diffusion chamber for ice nucleation studies. *Atmospheric Research*, *22*(2), 149–181. https://doi.org/10.1016/0169-8095(88)90005-1

Rogers, D. C., DeMott, P. J., Kreidenweis, S. M., & Chen, Y. (1998). Measurements of ice nucleating aerosols during SUCCESS. *Geophysical Research Letters*, *25*(9), 1383–1386. https://doi.org/10.1029/97GL03478

Rogers, D. C., DeMott, P. J., Kreidenweis, S. M., & Chen, Y. (2001). A continuous-flow diffusion chamber for airborne measurements of ice nuclei. *Journal of Atmospheric and Oceanic Technology*, *18*(5), 725–741. https://doi.org/10.1175/1520-0426(2001)018<0725:ACFDCF>2.0.CO;2

Rogers, R. R., & Yau, M. K. (1989). A short course in cloud physics, Pergamon.

Santachiara, G., Matteo, L. D., Prodi, F., & Belosi, F. (2010). Atmospheric particles acting as ice forming nuclei in different size ranges. *Atmospheric Research*, *96*(2–3), 266–272. https://doi.org/10.1016/j.atmosres.2009.08.004

Schrod, J., Weber, D., Drücke, J., Keleshis, C., Pikridas, M., Ebert, M., et al. (2017). Ice nucleating particles over the eastern Mediterranean measured by unmanned aircraft systems. *Atmospheric Chemistry and Physics*, *17*(7), 4817–4835. https://doi.org/10.5194/acp-17-4817-2017

Seifert, P., Ansmann, A., Groβ, S., Freudenthaler, V., Heinold, B., Hiebsch, A., et al. (2011). Ice formation in ash-influenced clouds after the eruption of the Eyjafjallajökull volcano in April 2010. *Journal of Geophysical Research*, *116*, D00U04. https://doi.org/10.1029/2011JD015702

Seinfeld, J. H., & Pandis, S. N. (2016). *Atmospheric chemistry and physics: From air pollution to climate change*. Hoboken, NJ: John Wiley.

Sioutas, C., Koutrakis, P., Ferguson, S. T., & Burton, R. M. (1995). Development and evaluation of a prototype ambient particle concentrator for inhalation exposure studies. *Inhalation Toxicology*, *7*(5), 633–644. https://doi.org/10.3109/08958379509014470

Steinbacher, M., Wyss, S., Emmenegger, L., & Hüglin, C. (2016). National Air Pollution Monitoring Network (NABEL), *International Foundation HFJG, annual report*.

Stith, J. L., Ramanathan, V., Cooper, W. A., Roberts, G. C., Demott, P. J., Carmichael, G., et al. (2009). An overview of aircraft observations from the Pacific Dust Experiment campaign. *Journal of Geophysical Research*, *114*, D05207. https://doi.org/10.1029/2008JD010924

Stohl, A., Forster, C., Frank, A., Seibert, P., & Wotawa, G. (2005). Technical note: The Lagrangian particle dispersion model FLEXPART version 6.2. *Atmospheric Chemistry and Physics*, *5*, 2461–2474.

Stopelli, E., Conen, F., Morris, C. E., Herrmann, E., Bukowiecki, N., & Alewell, C. (2015). Ice nucleation active particles are efficiently removed by precipitating clouds. *Scientific Reports*, *5*(1), 16433. https://doi.org/10.1038/srep16433

Stull, R. B. (1988). *An introduction to boundary layer meteorology* Netherlands: Springer. https://doi.org/10.1007/978-94-009-3027-8

Sturm, P., Tuzson, B., Henne, S., & Emmenegger, L. (2013). Tracking isotopic signatures of CO_2 at the high altitude site Jungfraujoch with laser spectroscopy: Analytical improvements and representative results. *Atmospheric Measurement Techniques*, *6*, 1659–1671.

Sullivan, R. C., Petters, M. D., DeMott, P. J., Kreidenweis, S. M., Wex, H., Niedermeier, D., et al. (2010). Irreversible loss of ice nucleation active sites in mineral dust particles caused by sulphuric acid condensation. *Atmospheric Chemistry and Physics*, *10*(23), 11,471–11,487. https://doi.org/10.5194/acp-10-11471-2010

Turekian, K. K. (1968). Oceans, Prentice-Hall.

Vergara-Temprado, J., Murray, B. J., Wilson, T. W., O'Sullivan, D., Browse, J., Pringle, K. J., et al. (2017). Contribution of feldspar and marine organic aerosols to global ice nucleating particle concentrations. *Atmospheric Chemistry and Physics*, *17*(5), 3637–3658. https://doi.org/10.5194/acp-17-3637-2017

Weingartner, E., Nyeki, S., & Baltensperger, U. (1999). Seasonal and diurnal variation of aerosol size distributions ($10 < D < 750$ nm) at a high-alpine site (Jungfraujoch 3580 m asl). *Journal of Geophysical Research*, *104*(D21), 26,809–26,820. https://doi.org/10.1029/1999JD900170

Westbrook, C. D., & Illingworth, A. J. (2013). The formation of ice in a long-lived supercooled layer cloud. *Quarterly Journal of the Royal Meteorological Society*, *139*(677), 2209–2221. https://doi.org/10.1002/qj.2096

Wilson, T. W., Ladino, L. A., Alpert, P. A., Breckels, M. N., Brooks, I. M., Browse, J., et al. (2015). A marine biogenic source of atmospheric ice-nucleating particles. *Nature*, *525*(7568), 234–238. https://doi.org/10.1038/nature14986

Zanis, P., Ganser, A., Zellweger, C., Henne, S., Steinbacher, M., & Staehelin, J. (2007). Seasonal variability of measured ozone production efficiencies in the lower free troposphere of Central Europe. *Atmospheric Chemistry and Physics*, *7*(1), 223–236. https://doi.org/10.5194/acp-7-223-2007

Zellweger, C., Forrer, J., Hofer, P., Nyeki, S., Schwarzenbach, B., Weingartner, E., et al. (2003). Partitioning of reactive nitrogen (NOy) and dependence on meteorological conditions in the lower free troposphere. *Atmospheric Chemistry and Physics*, *3*(3), 779–796. https://doi.org/10.5194/acp-3-779-2003

Zipori, A., Rosenfeld, D., Shpund, J., Steinberg, D. M., & Erel, Y. (2012). Targeting and impacts of AgI cloud seeding based on rain chemical composition and cloud top phase characterization. *Atmospheric Research*, *114-115*, 119–130. https://doi.org/10.1016/j.atmosres.2012.05.023

Zipori, A., Rosenfeld, D., Tirosh, O., Teutsch, N., & Erel, Y. (2015). Effects of aerosol sources and chemical compositions on cloud drop sizes and glaciation temperatures. *Journal of Geophysical Research: Atmospheres*, *120*, 9653–9669. https://doi.org/10.1002/2015JD023270